

This work was written as part of one of the author's official duties as an Employee of the United States Government and is therefore a work of the United States Government. In accordance with 17 U.S.C. 105, no copyright protection is available for such works under U.S. Law.

Public Domain Mark 1.0

<https://creativecommons.org/publicdomain/mark/1.0/>

Access to this work was provided by the University of Maryland, Baltimore County (UMBC) ScholarWorks@UMBC digital repository on the Maryland Shared Open Access (MD-SOAR) platform.

Please provide feedback

Please support the ScholarWorks@UMBC repository by emailing scholarworks-group@umbc.edu and telling us what having access to this work means to you and why it's important to you. Thank you.

Aerosol Atmospheric Rivers as Drivers of Extreme Poor Air Quality Events and Record PM_{2.5} Levels

Sudip Chakraborty¹, Bin Guan², Duane Edward Waliser³, Arlindo M. daSilva⁴, and Jonathan H Jiang⁵

¹Jet Propulsion Laboratory

²UCLA

³JPL/Caltech

⁴NASA GSFC

⁵Jet Propulsion Laboratory, California Institute of Technology

November 14, 2023

Abstract

This study investigates the impacts of aerosol atmospheric rivers (AARs) on extreme Particulate Matter 2.5 (PM_{2.5}) levels (PM_{2.5} > 15mgm⁻³, as per the WHO) and on aerosol optical depth (AOD) extremes (AOD > 98th percentile) over the US and the globe, respectively, between 1997-2020. Results show that over various regions over the US, extreme PM_{2.5} values are associated with AARs up to 70% of the time. Dust (sulfate) AARs are responsible for extreme PM_{2.5} levels over the southwestern (northeastern and the east coastal) US. Organic and black carbon AARs are associated with extreme PM_{2.5} levels over the Midwest region of the US. Globally, AARs are associated with 40-80% of the extreme AOD levels over the US, Sahel, Europe, Middle East, US, South America, East Asia, India, and South Africa. Such associations often lead to the highest or the second highest PM_{2.5} and AOD levels recorded over those stations between 1997-2020.

Aerosol Atmospheric Rivers as Drivers of Extreme Poor Air Quality Events and Record PM_{2.5} Levels

Sudip Chakraborty^{1*}, Bin Guan^{1,2}, Duane E. Waliser¹, Arlindo M. da Silva³, Jonathan H Jiang¹

¹Jet Propulsion Laboratory, California Institute of Technology, Pasadena, CA, USA

²Joint Institute for Regional Earth System Science and Engineering, University of California, Los Angeles, CA, USA

³ Global Modeling and Assimilation Office, NASA/Goddard Space Flight Center, Greenbelt, MD, USA

*Corresponding Author email: ; Bin.Guan@jpl.nasa.gov

Abstract

This study investigates the impacts of aerosol atmospheric rivers (AARs) on extreme Particulate Matter 2.5 (PM_{2.5}) levels (PM_{2.5} > 15mgm⁻³, as per the WHO) and on aerosol optical depth (AOD) extremes (AOD > 98th percentile) over the US and the globe, respectively, between 1997-2020. Results show that over various regions over the US, extreme PM_{2.5} values are associated with AARs up to 70% of the time. Dust (sulfate) AARs are responsible for extreme PM_{2.5} levels over the southwestern (northeastern and the east coastal) US. Organic and black carbon AARs are associated with extreme PM_{2.5} levels over the Midwest region of the US. Globally, AARs are associated with 40-80% of the extreme AOD levels over the US, Sahel, Europe, Middle East, US, South America, East Asia, India, and South Africa. Such associations often lead to the highest or the second highest PM_{2.5} and AOD levels recorded over those stations between 1997-2020.

Plain Language Summary

Particulate matters with a diameter less than 2.5μ (i.e., $PM_{2.5}$) have a deleterious impact on human health, especially on the respiratory system, including causing millions of premature deaths every year. This study finds out that long-range extreme transport of aerosols by aerosol atmospheric rivers (AARs) can be associated up to 70% of the time with extreme $PM_{2.5}$ levels over the Midwestern, southwestern, and eastern US and with high aerosol optical depth (AOD) over many regions in Europe, East Asia, South America, and Africa. This study points out the impact of AARs on global air quality.

Introduction

Air pollution has significant impacts on the respiratory system and can exacerbate several fatal conditions, such as heart disease, stroke, chronic obstructive pulmonary disease, cancer, and pneumonia (<https://www.who.int/data/gho/data/themes/theme-details/GHO/air-pollution>). Each year, according to the World Health Organization (WHO), 2.4 billion people are exposed to poor ambient and even indoor air quality that result in 7 million premature deaths (https://www.who.int/health-topics/air-pollution#tab=tab_2) – a much higher number than the ongoing COVID -19 related deaths or infections (<https://coronavirus.jhu.edu/data>).

Atmospheric particulate matter (PM) is one of the major culprits among the pollutants contributing to the poor air quality events and consist of organic and inorganic mixtures of liquid and solid-state sulfate, nitrates, mineral dust, ammonia, black carbon, and water (Ye et al., 2003). Those with a diameter less than 2.5 microns ($PM_{2.5}$) are especially dangerous to the lungs as they can penetrate the lung barrier, damage the alveolar wall, impair lung function (Xing et al., 2016), enter the bloodstream, and cause human mortality (Apte et al., 2015; R. Li et al., 2018; Xing et al., 2016). The sources of $PM_{2.5}$ can be local emissions (Guo et al., 2019; Zíková et al., 2016) as well as long-range transport of aerosols (Bae et al., 2020; D. Li et al., 2017; Perrone et al., 2013; Saliba et al., 2007; Squizzato et al., 2012; Wang et al., 2015). The source-receptor relationship of long-range aerosol transport (Clappier et al., 2015) on air quality and $PM_{2.5}$ related health impacts has been often studied (Kong et al., 2010; Todorović et al., 2020). Such studies have used observations (Uranishi et al., 2019; Wang et al., 2015) and models (Chen et al., 2014; Kong et al., 2010; Shimadera et al., 2016) to understand the impact of long-range aerosol transport on the air quality events and $PM_{2.5}$ level over various receptor regions of the world (Bae et al., 2020;

Chen et al., 2014; Guo et al., 2019; Kong et al., 2010; D. Li et al., 2017; Perrone et al., 2013; Saliba et al., 2007; Shimadera et al., 2016; Squizzato et al., 2012; Zíková et al., 2016). However, a clear picture of the role of long-range transport, especially the extreme transport events, on a global scale in affecting the local values of aerosol concentration and PM_{2.5} level is still lacking, primarily due to the lack of studies using long-record information about aerosol transports and their impacts on air quality. A proper understanding of how long-range aerosol transport can elevate PM_{2.5} levels is warranted.

Applying the atmospheric river concept for water vapor (Guan et al., 2020; Guan & Waliser, 2015) to aerosols (Chakraborty et al., 2021, 2022), it has been found that aerosols are also transported through narrow and elongated (longer than 2000 km) channels of atmospheric flow – referred to as aerosol atmospheric rivers (AARs) (Chakraborty et al., 2021, 2022). Annually, 30-40 AAR days contribute up to 80% of the dust (DU) transport and up to 40-50% of the sulfate (SU), organic carbon (OC), and black carbon (BC) aerosol transports (Chakraborty et al., 2021, 2022). But such transports are located over certain major transport pathways over the globe involving high aerosol-emitting source regions and the wind circulations picking up and transporting the aerosols to receptor regions (Chakraborty et al., 2021). AARs, by definition, contain a very high integrated aerosol transport (IAT) with a much higher mean aerosol mass mixing ratio within them than the non-AAR transport events (Chakraborty et al., 2021). Thus, it is crucial and very important to investigate how AARs have impacted the air quality and PM_{2.5} levels over time in various regions of the world.

With the above motivations, this study aims to clarify the role of AARs in establishing poor air quality events over various regions of the world. An AAR event database extending between 1997-2020 has been created using the Modern-Era Retrospective analysis for Research

and Applications (MERRA-2) which includes aerosol quantities, and has been used for scientific studies and is well-validated against the ground-based and satellite observations (Aldabash et al., 2020; Buchard et al., 2017; Global Modeling and Assimilation Office, 2015b, 2015a; Gueymard & Yang, 2020; Randles et al., 2017; Sitnov et al., 2020; Xu et al., 2020). Using in-situ measurements of $PM_{2.5}$ along with this database of AAR events, we will investigate the fractional contribution of AARs to extreme $PM_{2.5}$ levels, including top-ranked $PM_{2.5}$ events, over the US and extend the analysis to the association of AARs with extreme high aerosol optical depth (AOD) levels over various other regions of the world. $PM_{2.5}$ is measured at stations from the Interagency Monitoring of Protected Visual Environments (IMPROVE) network, which has been validated and used for scientific studies (Hwang & Hopke, 2007; Qiao et al., 2021; Solomon et al., 2014; Sorek-Hamer et al., 2013) over the US. Owing to the fact that the $PM_{2.5}$ measurements are not available over various locations across the globe, we will use in-situ measurements of AOD (Aldabash et al., 2020; Balarabe et al., 2015; Eck et al., 2005; Gueymard & Yang, 2020; Holben et al., 1998) from various Aerosol Robotic Network (Holben et al., 1998) (AERONET) stations as well as the AOD values from the MERRA-2 analysis. The former provides sparse but more accurate in-situ values while the latter provides more uncertain values but with complete spatial coverage over the globe. Please see the Methods section for the datasets used (Buchard et al., 2017; Global Modeling and Assimilation Office, 2015b, 2015a; Randles et al., 2017) and how to calculate the associations between AARs and poor air quality events.

AARs and the elevated $PM_{2.5}$ levels over the US

Figure 1 shows examples of the impact of AARs on the $PM_{2.5}$ levels. Wildfires over California generated many SU and carbonaceous (OC and BC) AARs in September 2020. Figure

1A shows the locations of four major fires that burned areas of more than 15000 acres and lasted more than two months – the Creek fire, the El Dorado fire, the Bobcat fire, and the Slater-Devil fire that started on 9/4, 9/5, 9/6, and 9/7, respectively. Our algorithm detects one SU AAR on September 12th (Fig. S1A) that reached far from the wildfire source regions over to the Midwest US and Canada on September 13th (Fig. 1A). The river continued to propagate eastward and was joined by another SU river traveling across the Pacific Ocean, resulting in an increase in the IAT value of the AAR (see vectors, Fig. 1B). The AAR heavily impacted the air quality over the regions crossed over (Fig.1C). The Kalmiopsis station monitoring the PM_{2.5} level over Oregon exhibited a huge increase in the PM_{2.5} level from 10 μ on 9/6 to 186 μgm^{-3} on 9/12. It is also important to note that the daily limit of PM_{2.5} exposure by the World Health Organization is 15 μgm^{-3} ([https://www.who.int/news-room/fact-sheets/detail/ambient-\(outdoor\)-air-quality-and-health](https://www.who.int/news-room/fact-sheets/detail/ambient-(outdoor)-air-quality-and-health)). The AAR also impacted the PM_{2.5} levels over regions far from where it originated. The AAR raised the PM_{2.5} level ($\sim 80\mu\text{gm}^{-3}$; rank=1) over the North Cascades station in Washington on 9/12. The Gates of the Mountains station in Montana, being located east of the wildfire region, recorded a peak in the PM_{2.5} level ($\sim 75\mu\text{gm}^{-3}$; rank=1) on 9/15. The AAR left the northwestern US on the next day (9/15; Fig. S1B) and moved to the east with these northwestern US stations experiencing a decline in the PM_{2.5} levels after 9/15.

It has also been noted that the poor air quality events and elevated PM_{2.5} levels can also be caused by many inter-continental transport events (Han et al., 2015; Karaca et al., 2009; Lin et al., 2005; Perrone et al., 2013; Prospero, 1999; Wang et al., 2015). Figures 1D-1F show one example of the impact of a DU AAR on the PM_{2.5} level over a station in Minnesota. The DU AAR originated from east Asia traveled over the Pacific Ocean and reached north America on 9/1/2011 (Fig. S2A). The AAR continued to transport dust over Canada and the northern US for

a week (Fig. 1D). As a result, the PM_{2.5} monitoring station in the Boundary Waters Canoe Area, MN observed a rise in the PM_{2.5} level from 9/3 and recorded a maximum of $\sim 70 \mu\text{gm}^{-3}$ (rank =1) on 9/12 (Fig. 1F) when the tail of the AAR reached the station (Fig. 1E). The AAR split on 9/12 at 1800 UTC and left the region (Fig. S2B). As a result, the PM_{2.5} level dropped below the WHO limit on 9/15.

These case studies show the impact of the wildfire and the dust emissions by the anomalous wind circulation on poor air quality conditions over regions far from their source regions – often inter-continental. Before further illustrating the impacts of AARs on local US or global air quality, we show the AAR climatologies and identify the major transport pathways of DU, SU, OC, and BC AARs between 1997-2020. Figure 2 shows the annual mean frequency of AAR occurrences by species in days per year. Figure 2A shows that the global deserts give rise to 30-40 DU AAR days each year. The major transport pathways are located between the Sahara Desert to the North Atlantic Ocean and the Sahara Desert to Europe and the middle east region. Numerous DU AARs are located over China, Mongolia, and Kazakhstan. In the Southern Hemisphere, many DU AARs originate from the Atacama, Kalahari, and Patagonia Deserts. Figure 2B shows that SU AARs are more frequent (~ 40 days/year, Fig. 2B) in the Northern Hemisphere than in the Southern Hemisphere owing to the emissions of SO₂ from biogenic and anthropogenic activities over China, Europe, and the eastern US (Chakraborty et al., 2022). In the Southern Hemisphere, major transport pathways of SU AARs include regions from the southern edges of the global rainforests to the South Indian, South Atlantic, and Southern Oceans. Global rainforests and boreal forests form many BC and OC rivers due to biomass burning (Figs. 2C and 2D). Other regions of high AAR activities are noted over the

industrialized areas over eastern China, north India, Europe, eastern US where 20-40 BC or OC AAR days are observed annually.

To illustrate the overall impacts of AARs on the $PM_{2.5}$ levels over the US, we use the $PM_{2.5}$ measurements of the IMPROVE network between 1997-2020. Figure 3A-3D show the fraction of the time when AARs are associated with extreme $PM_{2.5}$ over various stations in the US. Here, extremes are defined as $PM_{2.5}$ concentration over a station greater than $15\mu g m^{-3}$. Figure 3A shows that the DU AARs are associated ~20% of the extreme $PM_{2.5}$ values over most of the US, except in the southwest US over Arizona, New Mexico, Colorado, and Utah where the association can be as high as 50% – presumably because of the DU AARs are at least in part generated from the desert and drylands in these regions. Over the stations located west of the Rocky Mountains, SU AARs are associated 20-50% of the extreme $PM_{2.5}$ values. However, the association increases to 30-70% over the stations east of the Rocky Mountain because many of the SU AARs are generated over the eastern US (Fig. 2B). OC and BC AARs are also responsible for poor air quality events, up to 70% of the extreme $PM_{2.5}$ values exhibited by the stations in the Midwest US. Apart from those generated over the US due to wildfire as shown in Figure 1, many OC and BC AARs travel from Asia (Fig. 2C and 2D) and can degrade US air quality. OC and BC AARs are strongly (up to 70%) associated with poor air quality events over stations located in the Midwest US region, where the anthropogenic and industrial emission is less. On the other hand, stations located over the west coast show a lower association (~10-20%, except ~50% in Los Angeles) between extreme $PM_{2.5}$ values and OC and BC AARs. This indicates that the high $PM_{2.5}$ levels over there are due to local emissions from industrial activities and anthropogenic emissions from the major cities located in the west coast region rather than long-range transport.

In order to explore the relationship between AARs and PM_{2.5} levels, we evaluate the ranking of the extreme PM_{2.5} levels (shading) and associated PM_{2.5} values (bubble size) over these stations. Figure 3E shows that few stations over the Southwest US, where the association between DU AARs and PM_{2.5} level was observed to be higher, are identified with red bubbles - denoting that AARs are associated with the strongest (rank 1) or the second strongest (rank 2) PM_{2.5} values recorded during the analysis period over those stations (Note that the daily PM_{2.5} records consist of 104 values or more). Stations with orange (green) colored bubble indicates the AARs were associated with the third strongest to the fifth strongest or rank 3-5 (sixth highest to ninth highest or rank 6-9) PM_{2.5} values recorded by those stations. Most of the stations in the US show that the DU AARs are associated with ranks weaker than 9 - similar to the weaker association between DU AARs and the PM_{2.5} levels.

Our results show that the ranking of SU, OC, and BC AARs with the elevated PM_{2.5} levels is stronger than that of DU AARs (Figs. 3F-3H). Although the overall association between SU AARs and high PM_{2.5} levels is weak over the regions west of the Rocky Mountains (Fig. 3B), the association tends to produce the top-ranked PM_{2.5} levels there (red bubbles, Fig. 3F). The SU AAR-associated PM_{2.5} levels are also top-ranked over the states over the eastern US, where the overall association between SU AARs and PM_{2.5} levels is strong. The size of the bubbles denotes the corresponding extreme PM_{2.5} values at that rank. For example, the bubble size over the Kalmiopsis station in Oregon shows the highest ever recorded PM_{2.5} value (186 μgm^{-3} , rank =1) over the US as shown in the case study (Fig. 1C). OC and BC AARs are often associated with the strongest or the second strongest PM_{2.5} values over most of the stations located on the west coast, Midwest, southwest, and east coast of the US (Fig. 3G and 3H).

AARs and the elevated AOD levels over the globe

In order to get a global picture of the relationships between AARs and poor air quality events, we analyze the association of the extremely high ($\text{AOD} > 98^{\text{th}}$ percentile between 1997-2020) fine (Fig. 4) and coarse (Fig. S4) mode (O'Neill et al., 2003) AOD values observed over various AERONET stations, since the availability of PM_{2.5} measurements over the globe is scarce. See Figure S3 for the 98th percentile limits of fine and coarse mode AOD values between 1997-2020. Stations with at least 10 years of level 2 data between 1997-2020 have been included in the analysis. The association of DU AARs with extreme fine-mode AOD values is relatively weak (~20%) over most of the stations except the Sahel and the Caribbean regions, where the association can reach up to 80%. In addition, the association is very high (~80%) over the Sahel and the Caribbean regions, Europe, and east Asia when we consider extreme coarse-mode AOD values (Fig. S4A). On the other hand, SU AARs are often associated (40-80%) with high fine-mode AOD values over many regions of the world, such as the eastern US, Europe, and east Asia (Fig. 4B). For extreme fine-mode AOD values, OC and BC aerosols have the highest association over various regions of the globe (Figs. 4C-4D). Such regions include the western US, east coast of the US, Amazonia, the south African region as well as Madagascar, the Ascension Island (because of the AARs generated from the Congo rainforest; Figs. 2C and 2D) in the tropical Atlantic Ocean, and east Asia. On the contrary, the association of SU, OC, and BC AARs with high coarse-mode AOD values is weaker (Figs. S4B-S4D). The size of the bubbles represents the average number of AARs observed per year between 1997-2020 over the stations shown in Figure 2.

Although DU AARs are not frequently associated with extreme fine-mode AOD values, the DU AAR-associated fine-mode AOD values attain the top ranks (rank 1 or 2) over many regions of the world including the eastern US, western Europe, Sahel region, south African countries,

and Japan (Fig. 4E). For coarse-mode AOD, the ranks are stronger over almost entire European continent, the middle-east region, east Asia, Indian subcontinent, and the Caribbean region (Fig. S5A). The red bubbles in Figures 4B-4D show that SU, OC, and BC AARs occupy the strongest ranks over almost all the stations in the world.

We also compare the association of AARs and extreme AOD values from AERONET stations (bubbles), MERRA-2 (Fig. S6), and the Moderate Resolution Imaging Spectroradiometer or MODIS satellite (Fig. S7). Figure S7 shows a reasonable agreement between the association of AARs with high AERONET AOD (AOD_A , coarse mode for DU AARs and fine mode for others), high MODIS AOD (AOD_{MO}), and MERRA-2 AOD (AOD_{ME} , Fig. S6) over the AERONET stations and their surrounding regions. AOD_{ME} (Fig. S6) appears to be lower than AOD_{MO} (Fig. S7). Figure S8 shows associated biases, root mean squared errors (RMSE), Pearson's correlation coefficient, associated significant level (p values) between AOD_A (X-axis) and AOD_{MO} as well as AOD_{ME} (Y-axis) over the AERONET stations. AOD_{ME} and AOD_A have a higher correlation than that between AOD_{MO} and AOD_A for all the species of aerosols. However, AOD_{ME} shows higher biases for all the species. RMSE values are also higher for the AOD_{ME} for DU and OC AARs.

Socio-economic impacts

The objective of this study is to show the connection between the AAR's impacts by estimating the association and intensity (in terms of ranks) with the $PM_{2.5}$ levels, which is directly related to respiratory health, in the US. We also extend the study on a global perspective by using a proxy of aerosols - AOD measured over various in-situ AERONET stations. Our findings show the impact of AARs on the poor $PM_{2.5}$ and AOD levels over the United States and the globe, respectively. AARs significantly elevate the $PM_{2.5}$ levels over various locations in the

US and are associated with $PM_{2.5}$ values above the WHO daily limit (up to 70-80% of the time). AARs are associated with extremely high AOD levels over various locations around the globe. Such association can be as high as 80% of the time. Not only that, the top-ranked (rank 1-2) $PM_{2.5}$ and AOD levels for the whole records (1997-2020) are often associated with long-range transport by AARs. Over the US, the association and the rank of the AARs with the extreme $PM_{2.5}$ and AOD levels are in tandem with each other. For example, SU AARs have an overall stronger (weaker) association with the $PM_{2.5}$ (Fig. 3B) and AOD (Fig. 4B) levels over the eastern (western) US, but they produced the top-ranked events (rank 1-2) over both regions (Figs. 3F and 4F).

Such a strong association between AARs and extreme $PM_{2.5}$ /AOD occurrences and ranks found in our study show only 30-40 AAR days each year can have significant impacts on the air quality and visibility – factors that cause millions of deaths each year. Such poor air quality events due to long-range aerosol transport, often unnoticed to the people in the receptor region, can have severe impacts on the medical industries by causing them billions of dollars. For example, the 2019-2020 wildfire season in Australia caused smoke-related $PM_{2.5}$ induced health costs of AU\$1.95 billion. The real-time aerosol product using the nature run of the GOES FP system that provides analysis and forecast products can be used to detect the real-time AAR events. Thus, poor air quality warnings can be issued in real-time for AAR related elevated $PM_{2.5}$ events and precautionary measures can be used to prevent lung disease and deaths.

The interactions between the long-range aerosol transport and poor air quality events have been investigated before. However, to our knowledge, no other study shows the unique assessment and insight provided in this study on the association and the rank of the poor air quality events with long-range aerosol transports, especially using long-term datasets (i.e. 1997-

2020). The insights are extremely important since this study investigates the impacts coming from extreme aerosol transport events, or AARs that have a very high aerosol content compared to other transport events (Chakraborty et al., 2022) . The concept might also be useful and shows promises to further study the extreme air quality events associated with AARs. Future studies based on the database created for AARs (Chakraborty et al., 2021)

(<https://doi.org/10.25346/S6/CXO9PD>) can include the real-time air quality impacts due to AARs, investigating the health impacts and death related during such events, the role of local environmental factors on poor quality events and long-range transport as well local emissions, and the assessing the monetary impacts to the medical industries including the hospitals and the insurance companies. It is important to know that despite SU AARs also travel from the East Asian region like OC and BC AARs, they do not have a higher association with the $PM_{2.5}$ levels over the Midwest region like OC and BC AARs have. SU AARs have a higher association over the stations east of the Rocky Mountains – located relatively closer to the source region compared to those SU AARs travelling from East Asia to the Midwest region. Studies involving chemical analysis and aging are needed in the future to understand the reason behind that.

Methods

A widely used AR detecting algorithm has been modified to detect narrow and elongated regions of high IAT values associated with AARs. The AAR detection algorithm is applied to IAT from the MERRA-2 reanalysis (Buchard et al., 2017; Global Modeling and Assimilation Office, 2015b, 2015a; Randles et al., 2017). For $PM_{2.5}$ measurements from the IMPROVE network and cloud-screened version 2 AOD values from AERONET stations, we choose stations with at least 10 years of data between 1997-2020 since the AAR database ranges between 1997-2020. Both the datasets are well validated and have previously been used for scientific studies

(Aldabash et al., 2020; Balarabe et al., 2015; Eck et al., 2005; Gueymard & Yang, 2020; Hwang & Hopke, 2007; Qiao et al., 2021; Sorek-Hamer et al., 2013). We first extract the dates when $PM_{2.5}$ and AOD values are higher than the WHO daily limit and above the 98th percentiles of the AOD values between 1997-2020, respectively. Then we compute how many of those days AARs have been observed over the stations and compute the fractional association (η_{AAR}) as:

$$\eta_{AAR} = \eta_{AARdays}(PM_{2.5} > 15) / \eta_{days}(PM_{2.5} > 15)$$

The rank of the association is calculated by finding the position of the maximum $PM_{2.5}$ or AOD values during AAR days relative to the $PM_{2.5}$ or AOD values during all the data records. We have calculated a similar association between MODIS and MERRA-2 AOD at every grid point. We have used daily level 3 gridded MOD08 and version 2 (MODIS Science Team, 2014) of the MERRA-2 aerosol reanalysis (Gelaro et al., 2017) dataset for the AOD information. For details of the datasets used in this study, please see Table S1 in the supplementary section.

Acknowledgement

This work was supported by the National Aeronautics and Space Administration. The contribution of S.C. and D.W. was carried out on behalf of the Jet Propulsion Laboratory, California Institute of Technology, under a contract with NASA. No new dataset has been developed in this study. Also, details about the dataset have been included in the supplementary section.

Open Research

All the data are publicly available and free to download. The links to the datasets are provided here: MODIS (<https://modis.gsfc.nasa.gov/data/dataproduct/mod08.php>); MERRA-2 (https://disc.gsfc.nasa.gov/datasets/M2I3NXGAS_5.12.4/summary); AAR data (<https://doi.org/10.25346/S6/CXO9PD>); IMPROVE network data

(<http://views.cira.colostate.edu/fed/>); AERONET data (https://aeronet.gsfc.nasa.gov/cgi-bin/webtool_aod_v3).

References:

- Aldabash, M., Bektas Balcik, F., & Glantz, P. (2020). Validation of MODIS C6.1 and MERRA-2 AOD Using AERONET Observations: A Comparative Study over Turkey. *Atmosphere*, 11(9), 905. <https://doi.org/10.3390/atmos11090905>
- Apte, J. S., Marshall, J. D., Cohen, A. J., & Brauer, M. (2015). Addressing Global Mortality from Ambient PM_{2.5}. *Environmental Science & Technology*, 49(13), 8057–8066. <https://doi.org/10.1021/acs.est.5b01236>
- Bae, C., Kim, B.-U., Kim, H. C., Yoo, C., & Kim, S. (2020). Long-Range Transport Influence on Key Chemical Components of PM_{2.5} in the Seoul Metropolitan Area, South Korea, during the Years 2012–2016. *Atmosphere*, 11(1), 48. <https://doi.org/10.3390/atmos11010048>
- Balarabe, M., Abdullah, K., & Nawawi, M. (2015). Seasonal Variations of Aerosol Optical Properties and Identification of Different Aerosol Types Based on AERONET Data over Sub-Sahara West-Africa. *Atmospheric and Climate Sciences*, 6(1), 13–28. <https://doi.org/10.4236/acs.2016.61002>
- Bell, M. L., Dominici, F., Ebisu, K., Zeger, S. L., & Samet, J. M. (2007). Spatial and Temporal Variation in PM_{2.5} Chemical Composition in the United States for Health Effects Studies. *Environmental Health Perspectives*, 115(7), 989–995. <https://doi.org/10.1289/ehp.9621>
- Buchard, V., Randles, C. A., Silva, A. M. da, Darmenov, A., Colarco, P. R., Govindaraju, R., et al. (2017). The MERRA-2 Aerosol Reanalysis, 1980 Onward. Part II: Evaluation and Case Studies. *Journal of Climate*, 30(17), 6851–6872. <https://doi.org/10.1175/JCLI-D-16-0613.1>
- Chakraborty, S., Guan, B., Waliser, D. E., da Silva, A. M., Uluatam, S., & Hess, P. (2021). Extending the Atmospheric River Concept to Aerosols: Climate and Air Quality Impacts. *Geophysical Research Letters*, 48(9), e2020GL091827. <https://doi.org/10.1029/2020GL091827>
- Chakraborty, S., Guan, B., Waliser, D. E., & da Silva, A. M. (2022). Aerosol atmospheric rivers: climatology, event characteristics, and detection algorithm sensitivities. *Atmospheric Chemistry and Physics*, 22(12), 8175–8195. <https://doi.org/10.5194/acp-22-8175-2022>
- Chen, T.-F., Chang, K.-H., & Tsai, C.-Y. (2014). Modeling direct and indirect effect of long range transport on atmospheric PM_{2.5} levels. *Atmospheric Environment*, 89, 1–9. <https://doi.org/10.1016/j.atmosenv.2014.01.065>
- Clappier, A., Pisoni, E., & Thunis, P. (2015). A new approach to design source–receptor relationships for air quality modelling. *Environmental Modelling & Software*, 74, 66–74. <https://doi.org/10.1016/j.envsoft.2015.09.007>
- Eck, T. F., Holben, B. N., Dubovik, O., Smirnov, A., Goloub, P., Chen, H. B., et al. (2005). Columnar aerosol optical properties at AERONET sites in central eastern Asia and

- aerosol transport to the tropical mid-Pacific. *Journal of Geophysical Research: Atmospheres*, 110(D6). <https://doi.org/10.1029/2004JD005274>
- Gelaro, R., McCarty, W., Suárez, M. J., Todling, R., Molod, A., Takacs, L., et al. (2017). The Modern-Era Retrospective Analysis for Research and Applications, Version 2 (MERRA-2). *Journal of Climate*, 30(14), 5419–5454. <https://doi.org/10.1175/JCLI-D-16-0758.1>
- Global Modeling and Assimilation Office, G. (2015a). GES DISC Dataset: MERRA-2 tavg1_2d_aer_Nx: 2d,1-Hourly,Time-averaged,Single-Level,Assimilation,Aerosol Diagnostics V5.12.4 (M2T1NXAER 5.12.4). Retrieved April 20, 2023, from https://disc.gsfc.nasa.gov/datasets/M2T1NXAER_5.12.4/summary
- Global Modeling and Assimilation Office, G. (2015b). GES DISC Dataset: MERRA-2 tavgU_2d_adg_Nx: 2d,diurnal,Time-averaged,Single-Level,Assimilation,Aerosol Diagnostics (extended) V5.12.4 (M2TUNXADG 5.12.4). Retrieved April 20, 2023, from https://disc.gsfc.nasa.gov/datasets/M2TUNXADG_5.12.4/summary
- Guan, B., & Waliser, D. E. (2015). Detection of atmospheric rivers: Evaluation and application of an algorithm for global studies. *Journal of Geophysical Research: Atmospheres*, 120(24), 12514–12535. <https://doi.org/10.1002/2015JD024257>
- Guan, B., Waliser, D. E., & Ralph, F. M. (2020). A multimodel evaluation of the water vapor budget in atmospheric rivers. *Annals of the New York Academy of Sciences*, 1472(1), 139–154. <https://doi.org/10.1111/nyas.14368>
- Gueymard, C. A., & Yang, D. (2020). Worldwide validation of CAMS and MERRA-2 reanalysis aerosol optical depth products using 15 years of AERONET observations. *Atmospheric Environment*, 225, 117216. <https://doi.org/10.1016/j.atmosenv.2019.117216>
- Guo, H., Kota, S. H., Sahu, S. K., & Zhang, H. (2019). Contributions of local and regional sources to PM_{2.5} and its health effects in north India. *Atmospheric Environment*, 214, 116867. <https://doi.org/10.1016/j.atmosenv.2019.116867>
- Han, L., Cheng, S., Zhuang, G., Ning, H., Wang, H., Wei, W., & Zhao, X. (2015). The changes and long-range transport of PM_{2.5} in Beijing in the past decade. *Atmospheric Environment*, 110, 186–195. <https://doi.org/10.1016/j.atmosenv.2015.03.013>
- Holben, B. N., Eck, T. F., Slutsker, I., Tanré, D., Buis, J. P., Setzer, A., et al. (1998). AERONET—A Federated Instrument Network and Data Archive for Aerosol Characterization. *Remote Sensing of Environment*, 66(1), 1–16. [https://doi.org/10.1016/S0034-4257\(98\)00031-5](https://doi.org/10.1016/S0034-4257(98)00031-5)
- Hwang, I., & Hopke, P. K. (2007). Estimation of source apportionment and potential source locations of PM_{2.5} at a west coastal IMPROVE site. *Atmospheric Environment*, 41(3), 506–518. <https://doi.org/10.1016/j.atmosenv.2006.08.043>
- Karaca, F., Anil, I., & Alagha, O. (2009). Long-range potential source contributions of episodic aerosol events to PM₁₀ profile of a megacity. *Atmospheric Environment*, 43(36), 5713–5722. <https://doi.org/10.1016/j.atmosenv.2009.08.005>
- Kong, S., Han, B., Bai, Z., Chen, L., Shi, J., & Xu, Z. (2010). Receptor modeling of PM_{2.5}, PM₁₀ and TSP in different seasons and long-range transport analysis at a coastal site of Tianjin, China. *The Science of the Total Environment*, 408(20), 4681–4694. <https://doi.org/10.1016/j.scitotenv.2010.06.005>
- Lang, J., Zhang, Y., Zhou, Y., Cheng, S., Chen, D., Guo, X., et al. (2017). Trends of PM_{2.5} and Chemical Composition in Beijing, 2000–2015. *Aerosol and Air Quality Research*, 17(2), 412–425. <https://doi.org/10.4209/aaqr.2016.07.0307>

- Li, D., Liu, J., Zhang, J., Gui, H., Du, P., Yu, T., et al. (2017). Identification of long-range transport pathways and potential sources of PM_{2.5} and PM₁₀ in Beijing from 2014 to 2015. *Journal of Environmental Sciences (China)*, 56, 214–229. <https://doi.org/10.1016/j.jes.2016.06.035>
- Li, R., Zhou, R., & Zhang, J. (2018). Function of PM_{2.5} in the pathogenesis of lung cancer and chronic airway inflammatory diseases. *Oncology Letters*, 15(5), 7506–7514. <https://doi.org/10.3892/ol.2018.8355>
- Lin, C.-Y., Liu, S. C., Chou, C. C.-K., Huang, S.-J., Liu, C.-M., Kuo, C.-H., & Young, C.-Y. (2005). Long-range transport of aerosols and their impact on the air quality of Taiwan. *Atmospheric Environment*, 39(33), 6066–6076. <https://doi.org/10.1016/j.atmosenv.2005.06.046>
- MODIS Science Team. (2014). MYD08_M3 MODIS/Aqua Aerosol Cloud Water Vapor Ozone Monthly L3 Global 1Deg CMG [Data set]. NASA Level 1 and Atmosphere Archive and Distribution System. https://doi.org/10.5067/MODIS/MYD08_M3.006
- O'Neill, N. T., Eck, T. F., Smirnov, A., Holben, B. N., & Thulasiraman, S. (2003). Spectral discrimination of coarse and fine mode optical depth. *Journal of Geophysical Research (Atmospheres)*, 108, 4559. <https://doi.org/10.1029/2002JD002975>
- Perrone, M. R., Becagli, S., Garcia Orza, J. A., Vecchi, R., Dinoi, A., Udusti, R., & Cabello, M. (2013). The impact of long-range-transport on PM₁ and PM_{2.5} at a Central Mediterranean site. *Atmospheric Environment*, 71, 176–186. <https://doi.org/10.1016/j.atmosenv.2013.02.006>
- Prospero, J. M. (1999). Long-term measurements of the transport of African mineral dust to the southeastern United States: Implications for regional air quality. *Journal of Geophysical Research: Atmospheres*, 104(D13), 15917–15927. <https://doi.org/10.1029/1999JD900072>
- Qiao, X., Zhang, Q., Wang, D., Hao, J., & Jiang, J. (2021). Improving data reliability: A quality control practice for low-cost PM_{2.5} sensor network. *Science of The Total Environment*, 779, 146381. <https://doi.org/10.1016/j.scitotenv.2021.146381>
- Randles, C. A., Silva, A. M. da, Buchard, V., Colarco, P. R., Darmenov, A., Govindaraju, R., et al. (2017). The MERRA-2 Aerosol Reanalysis, 1980 Onward. Part I: System Description and Data Assimilation Evaluation. *Journal of Climate*, 30(17), 6823–6850. <https://doi.org/10.1175/JCLI-D-16-0609.1>
- Saliba, N. A., Kouyoumdjian, H., & Roumié, M. (2007). Effect of local and long-range transport emissions on the elemental composition of PM_{10-2.5} and PM_{2.5} in Beirut. *Atmospheric Environment*, 41(31), 6497–6509. <https://doi.org/10.1016/j.atmosenv.2007.04.032>
- Shimadera, H., Kojima, T., & Kondo, A. (2016). Evaluation of Air Quality Model Performance for Simulating Long-Range Transport and Local Pollution of PM_{2.5} in Japan. *Advances in Meteorology*, 2016, e5694251. <https://doi.org/10.1155/2016/5694251>
- Sitnov, S. A., Mokhov, I. I., & Likhoshesterova, A. A. (2020). Exploring large-scale black-carbon air pollution over Northern Eurasia in summer 2016 using MERRA-2 reanalysis data. *Atmospheric Research*, 235, 104763. <https://doi.org/10.1016/j.atmosres.2019.104763>
- Solomon, P. A., Crumpler, D., Flanagan, J. B., Jayanty, R. K. M., Rickman, E. E., & McDade, C. E. (2014). U.S. national PM_{2.5} Chemical Speciation Monitoring Networks-CSN and IMPROVE: description of networks. *Journal of the Air & Waste Management Association (1995)*, 64(12), 1410–1438. <https://doi.org/10.1080/10962247.2014.956904>
- Sorek-Hamer, M., Strawa, A. W., Chatfield, R. B., Esswein, R., Cohen, A., & Broday, D. M. (2013). Improved retrieval of PM_{2.5} from satellite data products using non-linear

- methods. *Environmental Pollution (Barking, Essex: 1987)*, 182, 417–423.
<https://doi.org/10.1016/j.envpol.2013.08.002>
- Squizzato, S., Masiol, M., Innocente, E., Pecorari, E., Rampazzo, G., & Pavoni, B. (2012). A procedure to assess local and long-range transport contributions to PM_{2.5} and secondary inorganic aerosol. *Journal of Aerosol Science*, 46, 64–76.
<https://doi.org/10.1016/j.jaerosci.2011.12.001>
- Todorović, M. N., Radenković, M. B., Onjia, A. E., & Ignjatović, L. M. (2020). Characterization of PM_{2.5} sources in a Belgrade suburban area: a multi-scale receptor-oriented approach. *Environmental Science and Pollution Research International*, 27(33), 41717–41730.
<https://doi.org/10.1007/s11356-020-10129-z>
- Uranishi, K., Ikemori, F., Shimadera, H., Kondo, A., & Sugata, S. (2019). Impact of field biomass burning on local pollution and long-range transport of PM_{2.5} in Northeast Asia. *Environmental Pollution*, 244, 414–422. <https://doi.org/10.1016/j.envpol.2018.09.061>
- Wang, L., Liu, Z., Sun, Y., Ji, D., & Wang, Y. (2015). Long-range transport and regional sources of PM_{2.5} in Beijing based on long-term observations from 2005 to 2010. *Atmospheric Research*, 157, 37–48. <https://doi.org/10.1016/j.atmosres.2014.12.003>
- Xing, Y.-F., Xu, Y.-H., Shi, M.-H., & Lian, Y.-X. (2016). The impact of PM_{2.5} on the human respiratory system. *Journal of Thoracic Disease*, 8(1), E69–E74.
<https://doi.org/10.3978/j.issn.2072-1439.2016.01.19>
- Xu, X., Wu, H., Yang, X., & Xie, L. (2020). Distribution and transport characteristics of dust aerosol over Tibetan Plateau and Taklimakan Desert in China using MERRA-2 and CALIPSO data. *Atmospheric Environment*, 237, 117670.
<https://doi.org/10.1016/j.atmosenv.2020.117670>
- Ye, B., Ji, X., Yang, H., Yao, X., Chan, C. K., Cadle, S. H., et al. (2003). Concentration and chemical composition of PM_{2.5} in Shanghai for a 1-year period. *Atmospheric Environment*, 37(4), 499–510. [https://doi.org/10.1016/S1352-2310\(02\)00918-4](https://doi.org/10.1016/S1352-2310(02)00918-4)
- Zíková, N., Wang, Y., Yang, F., Li, X., Tian, M., & Hopke, P. K. (2016). On the source contribution to Beijing PM_{2.5} concentrations. *Atmospheric Environment*, 134, 84–95.
<https://doi.org/10.1016/j.atmosenv.2016.03.047>

Figures

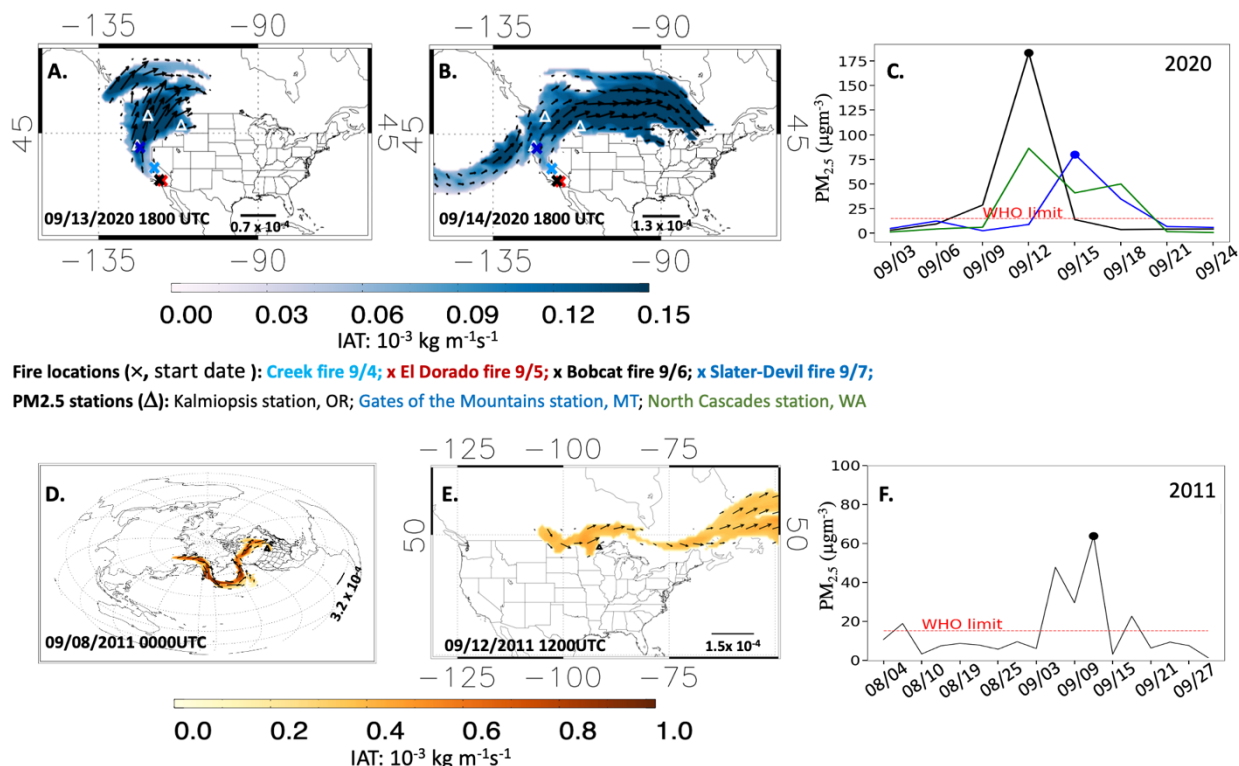


Figure1. Case studies of the impacts of AARs on PM_{2.5} levels. Figure 1 shows a Sulfate AAR generated from wild fire events in California. (A) The location of four large wildfire events with total burned area greater than 15000 acres and lasting for more than two months (marked in the map as x) on 09/13/2020 1800 UTC. The PM_{2.5} monitoring stations are marked as triangles. (B) The same river on 09/14/2020 at 1800 UTC. (C) PM_{2.5} levels monitored over the stations shown in the maps as triangles. (D) one dust AAR on 09/08/2011 at 00UTC. (E) The same river on 09/12/2011. (F) PM_{2.5} level monitored over the Boundary Water Canoe Area in MN (marked as triangle in the map) during the AAR event. Shading shows the IAT values and the arrows represent the vectors.

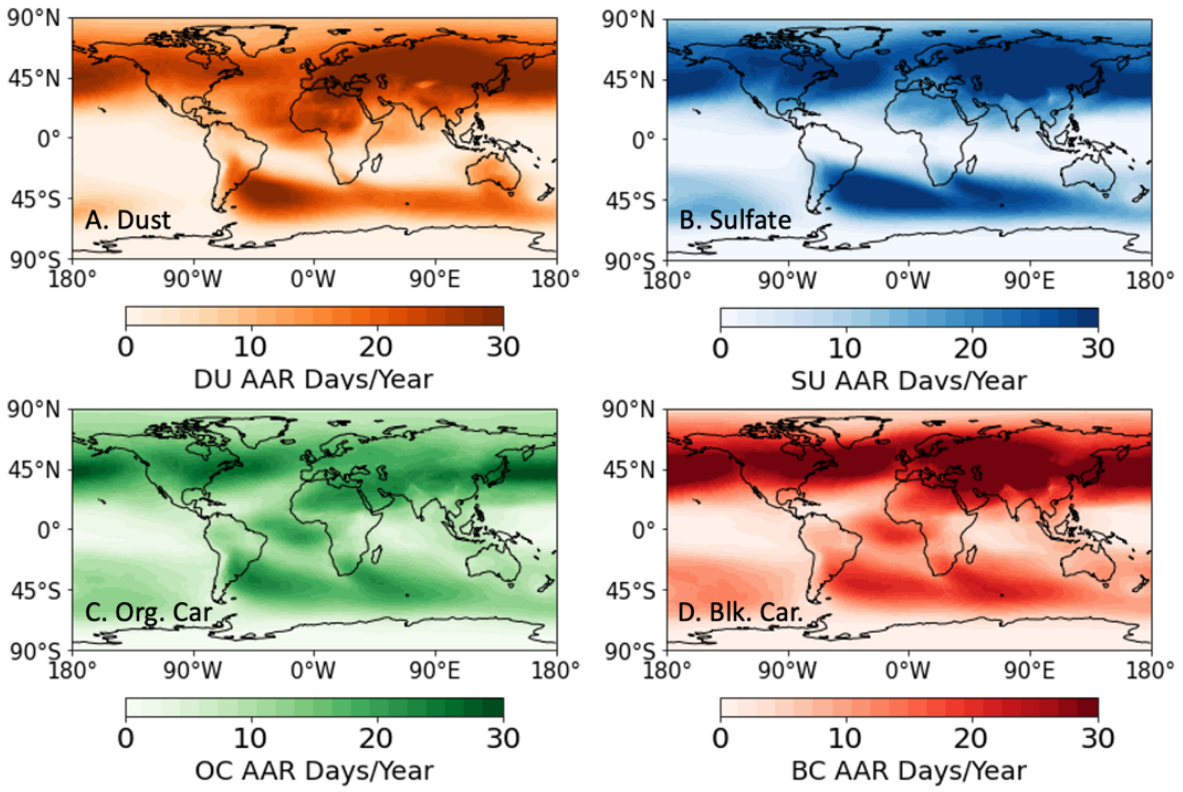


Figure 2. Maps of AAR days/year for four different species (A) dust, (B) sulfate, (C) organic carbon, and (D) black carbon between 1997-2020.

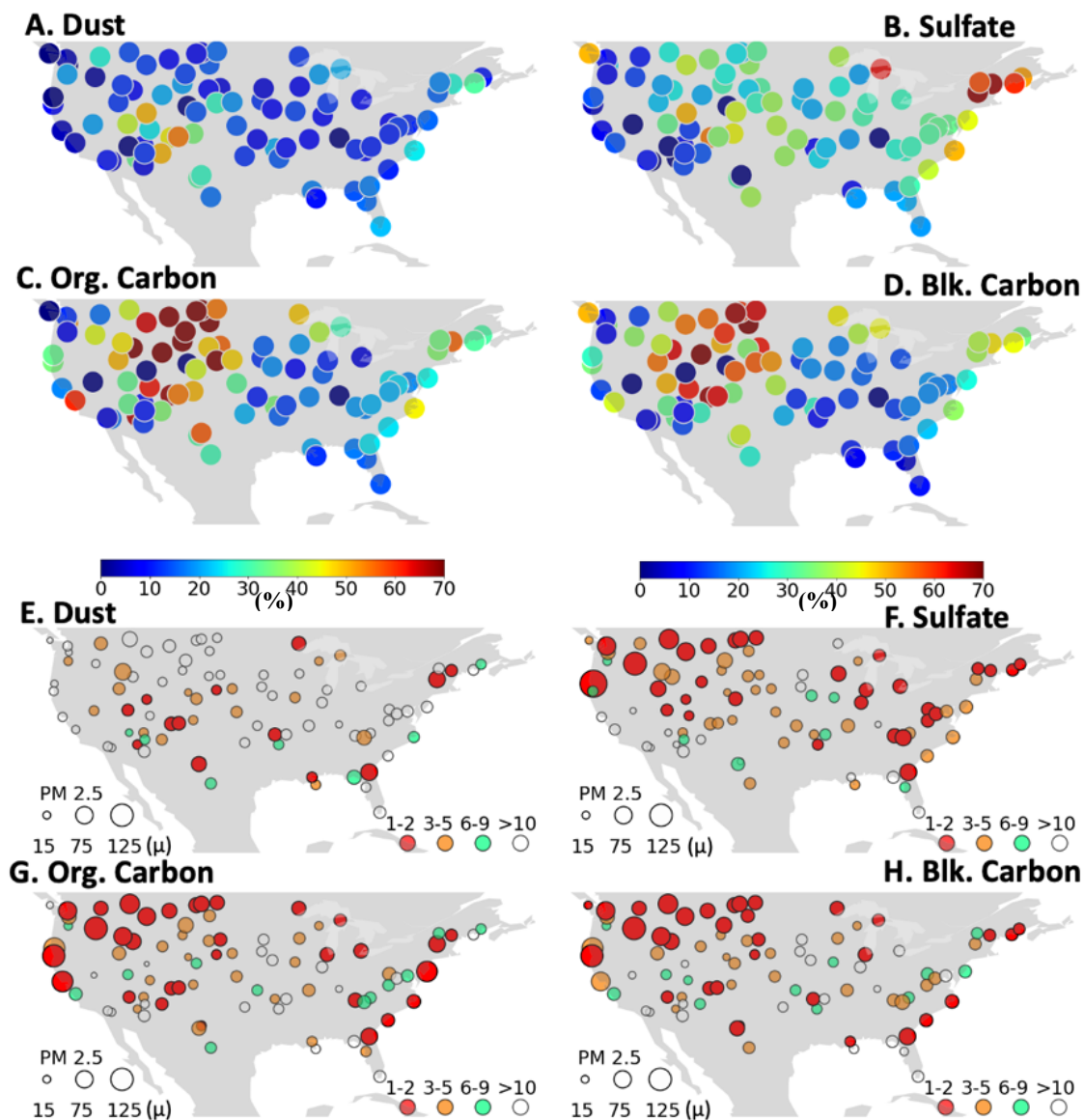


Figure 3. Fraction of extreme PM_{2.5} levels (PM_{2.5} > 15μ or WHO daily limit) associated with AAR events (shading, %) between 1997-2020 for (A) Dust, (B) Sulfate, (C) Organic Carbon, and (D) Black Carbon AARs. The highest rank (shading) of AAR related extremes associated with extreme PM_{2.5} levels for (E) Dust, (F) Sulfate, (G) Organic Carbon, and (H) Black Carbon AARs. The size of the circles shows the corresponding PM_{2.5} values at that rank.

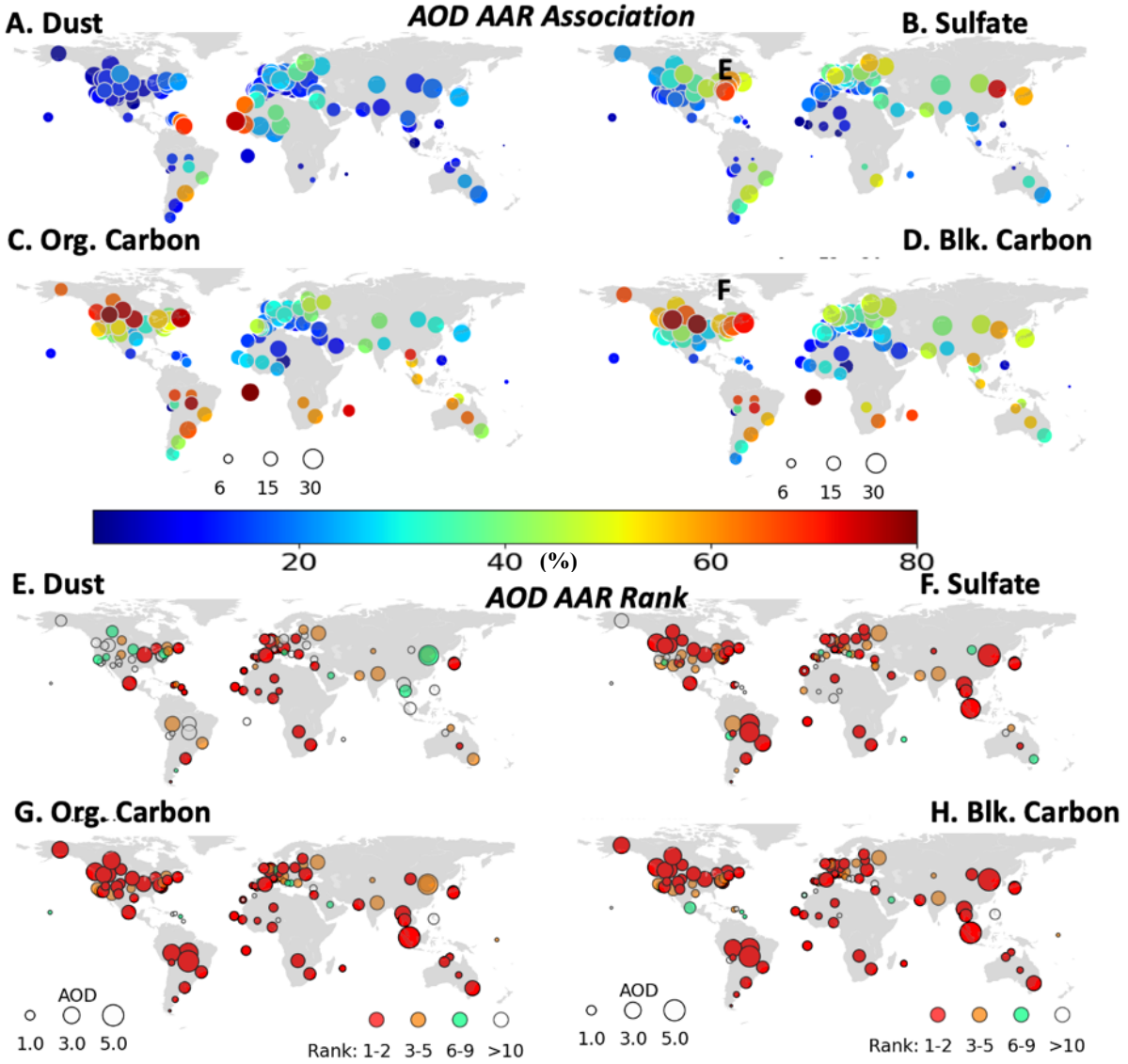


Figure 4. Fraction of extreme fine-mode AOD values ($\text{AOD} > 98^{\text{th}}$ percentile between 1997-2020) associated with AAR events (shading, %) and the AAR days/year (size of the bubbles) between 1997-2020 for (A) Dust, (B) Sulfate, (C) Organic Carbon, and (D) Black Carbon AARs. The size of the bubbles show the number of AARs observed each year over that station from Figure 2. The highest rank (shading) of AAR related extremes associated with extreme AOD values for (E) Dust, (F) Sulfate, (G) Organic Carbon, and (H) Black Carbon AARs. The size of the bubbles shows the corresponding AOD values at that rank.

Aerosol Atmospheric Rivers as Drivers of Extreme Poor Air Quality Events and Record PM_{2.5} Levels

Sudip Chakraborty^{1*}, Bin Guan^{1,2}, Duane E. Waliser¹, Arlindo M. da Silva³, Jonathan H Jiang¹

¹Jet Propulsion Laboratory, California Institute of Technology, Pasadena, CA, USA

²Joint Institute for Regional Earth System Science and Engineering, University of California, Los Angeles, CA, USA

³ Global Modeling and Assimilation Office, NASA/Goddard Space Flight Center, Greenbelt, MD, USA

*Corresponding Author email: ; Bin.Guan@jpl.nasa.gov

Abstract

This study investigates the impacts of aerosol atmospheric rivers (AARs) on extreme Particulate Matter 2.5 (PM_{2.5}) levels (PM_{2.5} > 15mgm⁻³, as per the WHO) and on aerosol optical depth (AOD) extremes (AOD > 98th percentile) over the US and the globe, respectively, between 1997-2020. Results show that over various regions over the US, extreme PM_{2.5} values are associated with AARs up to 70% of the time. Dust (sulfate) AARs are responsible for extreme PM_{2.5} levels over the southwestern (northeastern and the east coastal) US. Organic and black carbon AARs are associated with extreme PM_{2.5} levels over the Midwest region of the US. Globally, AARs are associated with 40-80% of the extreme AOD levels over the US, Sahel, Europe, Middle East, US, South America, East Asia, India, and South Africa. Such associations often lead to the highest or the second highest PM_{2.5} and AOD levels recorded over those stations between 1997-2020.

Plain Language Summary

Particulate matters with a diameter less than 2.5μ (i.e., $PM_{2.5}$) have a deleterious impact on human health, especially on the respiratory system, including causing millions of premature deaths every year. This study finds out that long-range extreme transport of aerosols by aerosol atmospheric rivers (AARs) can be associated up to 70% of the time with extreme $PM_{2.5}$ levels over the Midwestern, southwestern, and eastern US and with high aerosol optical depth (AOD) over many regions in Europe, East Asia, South America, and Africa. This study points out the impact of AARs on global air quality.

Introduction

Air pollution has significant impacts on the respiratory system and can exacerbate several fatal conditions, such as heart disease, stroke, chronic obstructive pulmonary disease, cancer, and pneumonia (<https://www.who.int/data/gho/data/themes/theme-details/GHO/air-pollution>). Each year, according to the World Health Organization (WHO), 2.4 billion people are exposed to poor ambient and even indoor air quality that result in 7 million premature deaths (https://www.who.int/health-topics/air-pollution#tab=tab_2) – a much higher number than the ongoing COVID -19 related deaths or infections (<https://coronavirus.jhu.edu/data>).

Atmospheric particulate matter (PM) is one of the major culprits among the pollutants contributing to the poor air quality events and consist of organic and inorganic mixtures of liquid and solid-state sulfate, nitrates, mineral dust, ammonia, black carbon, and water (Ye et al., 2003). Those with a diameter less than 2.5 microns ($PM_{2.5}$) are especially dangerous to the lungs as they can penetrate the lung barrier, damage the alveolar wall, impair lung function (Xing et al., 2016), enter the bloodstream, and cause human mortality (Apte et al., 2015; R. Li et al., 2018; Xing et al., 2016). The sources of $PM_{2.5}$ can be local emissions (Guo et al., 2019; Zíková et al., 2016) as well as long-range transport of aerosols (Bae et al., 2020; D. Li et al., 2017; Perrone et al., 2013; Saliba et al., 2007; Squizzato et al., 2012; Wang et al., 2015). The source-receptor relationship of long-range aerosol transport (Clappier et al., 2015) on air quality and $PM_{2.5}$ related health impacts has been often studied (Kong et al., 2010; Todorović et al., 2020). Such studies have used observations (Uranishi et al., 2019; Wang et al., 2015) and models (Chen et al., 2014; Kong et al., 2010; Shimadera et al., 2016) to understand the impact of long-range aerosol transport on the air quality events and $PM_{2.5}$ level over various receptor regions of the world (Bae et al., 2020;

Chen et al., 2014; Guo et al., 2019; Kong et al., 2010; D. Li et al., 2017; Perrone et al., 2013; Saliba et al., 2007; Shimadera et al., 2016; Squizzato et al., 2012; Zíková et al., 2016). However, a clear picture of the role of long-range transport, especially the extreme transport events, on a global scale in affecting the local values of aerosol concentration and PM_{2.5} level is still lacking, primarily due to the lack of studies using long-record information about aerosol transports and their impacts on air quality. A proper understanding of how long-range aerosol transport can elevate PM_{2.5} levels is warranted.

Applying the atmospheric river concept for water vapor (Guan et al., 2020; Guan & Waliser, 2015) to aerosols (Chakraborty et al., 2021, 2022), it has been found that aerosols are also transported through narrow and elongated (longer than 2000 km) channels of atmospheric flow – referred to as aerosol atmospheric rivers (AARs) (Chakraborty et al., 2021, 2022). Annually, 30-40 AAR days contribute up to 80% of the dust (DU) transport and up to 40-50% of the sulfate (SU), organic carbon (OC), and black carbon (BC) aerosol transports (Chakraborty et al., 2021, 2022). But such transports are located over certain major transport pathways over the globe involving high aerosol-emitting source regions and the wind circulations picking up and transporting the aerosols to receptor regions (Chakraborty et al., 2021). AARs, by definition, contain a very high integrated aerosol transport (IAT) with a much higher mean aerosol mass mixing ratio within them than the non-AAR transport events (Chakraborty et al., 2021). Thus, it is crucial and very important to investigate how AARs have impacted the air quality and PM_{2.5} levels over time in various regions of the world.

With the above motivations, this study aims to clarify the role of AARs in establishing poor air quality events over various regions of the world. An AAR event database extending between 1997-2020 has been created using the Modern-Era Retrospective analysis for Research

and Applications (MERRA-2) which includes aerosol quantities, and has been used for scientific studies and is well-validated against the ground-based and satellite observations (Aldabash et al., 2020; Buchard et al., 2017; Global Modeling and Assimilation Office, 2015b, 2015a; Gueymard & Yang, 2020; Randles et al., 2017; Sitnov et al., 2020; Xu et al., 2020). Using in-situ measurements of $PM_{2.5}$ along with this database of AAR events, we will investigate the fractional contribution of AARs to extreme $PM_{2.5}$ levels, including top-ranked $PM_{2.5}$ events, over the US and extend the analysis to the association of AARs with extreme high aerosol optical depth (AOD) levels over various other regions of the world. $PM_{2.5}$ is measured at stations from the Interagency Monitoring of Protected Visual Environments (IMPROVE) network, which has been validated and used for scientific studies (Hwang & Hopke, 2007; Qiao et al., 2021; Solomon et al., 2014; Sorek-Hamer et al., 2013) over the US. Owing to the fact that the $PM_{2.5}$ measurements are not available over various locations across the globe, we will use in-situ measurements of AOD (Aldabash et al., 2020; Balarabe et al., 2015; Eck et al., 2005; Gueymard & Yang, 2020; Holben et al., 1998) from various Aerosol Robotic Network (Holben et al., 1998) (AERONET) stations as well as the AOD values from the MERRA-2 analysis. The former provides sparse but more accurate in-situ values while the latter provides more uncertain values but with complete spatial coverage over the globe. Please see the Methods section for the datasets used (Buchard et al., 2017; Global Modeling and Assimilation Office, 2015b, 2015a; Randles et al., 2017) and how to calculate the associations between AARs and poor air quality events.

AARs and the elevated $PM_{2.5}$ levels over the US

Figure 1 shows examples of the impact of AARs on the $PM_{2.5}$ levels. Wildfires over California generated many SU and carbonaceous (OC and BC) AARs in September 2020. Figure

1A shows the locations of four major fires that burned areas of more than 15000 acres and lasted more than two months – the Creek fire, the El Dorado fire, the Bobcat fire, and the Slater-Devil fire that started on 9/4, 9/5, 9/6, and 9/7, respectively. Our algorithm detects one SU AAR on September 12th (Fig. S1A) that reached far from the wildfire source regions over to the Midwest US and Canada on September 13th (Fig. 1A). The river continued to propagate eastward and was joined by another SU river traveling across the Pacific Ocean, resulting in an increase in the IAT value of the AAR (see vectors, Fig. 1B). The AAR heavily impacted the air quality over the regions crossed over (Fig.1C). The Kalmiopsis station monitoring the PM_{2.5} level over Oregon exhibited a huge increase in the PM_{2.5} level from 10 μ on 9/6 to 186 μgm^{-3} on 9/12. It is also important to note that the daily limit of PM_{2.5} exposure by the World Health Organization is 15 μgm^{-3} ([https://www.who.int/news-room/fact-sheets/detail/ambient-\(outdoor\)-air-quality-and-health](https://www.who.int/news-room/fact-sheets/detail/ambient-(outdoor)-air-quality-and-health)). The AAR also impacted the PM_{2.5} levels over regions far from where it originated. The AAR raised the PM_{2.5} level ($\sim 80\mu\text{gm}^{-3}$; rank=1) over the North Cascades station in Washington on 9/12. The Gates of the Mountains station in Montana, being located east of the wildfire region, recorded a peak in the PM_{2.5} level ($\sim 75\mu\text{gm}^{-3}$; rank=1) on 9/15. The AAR left the northwestern US on the next day (9/15; Fig. S1B) and moved to the east with these northwestern US stations experiencing a decline in the PM_{2.5} levels after 9/15.

It has also been noted that the poor air quality events and elevated PM_{2.5} levels can also be caused by many inter-continental transport events (Han et al., 2015; Karaca et al., 2009; Lin et al., 2005; Perrone et al., 2013; Prospero, 1999; Wang et al., 2015). Figures 1D-1F show one example of the impact of a DU AAR on the PM_{2.5} level over a station in Minnesota. The DU AAR originated from east Asia traveled over the Pacific Ocean and reached north America on 9/1/2011 (Fig. S2A). The AAR continued to transport dust over Canada and the northern US for

a week (Fig. 1D). As a result, the PM_{2.5} monitoring station in the Boundary Waters Canoe Area, MN observed a rise in the PM_{2.5} level from 9/3 and recorded a maximum of $\sim 70 \mu\text{gm}^{-3}$ (rank =1) on 9/12 (Fig. 1F) when the tail of the AAR reached the station (Fig. 1E). The AAR split on 9/12 at 1800 UTC and left the region (Fig. S2B). As a result, the PM_{2.5} level dropped below the WHO limit on 9/15.

These case studies show the impact of the wildfire and the dust emissions by the anomalous wind circulation on poor air quality conditions over regions far from their source regions – often inter-continental. Before further illustrating the impacts of AARs on local US or global air quality, we show the AAR climatologies and identify the major transport pathways of DU, SU, OC, and BC AARs between 1997-2020. Figure 2 shows the annual mean frequency of AAR occurrences by species in days per year. Figure 2A shows that the global deserts give rise to 30-40 DU AAR days each year. The major transport pathways are located between the Sahara Desert to the North Atlantic Ocean and the Sahara Desert to Europe and the middle east region. Numerous DU AARs are located over China, Mongolia, and Kazakhstan. In the Southern Hemisphere, many DU AARs originate from the Atacama, Kalahari, and Patagonia Deserts. Figure 2B shows that SU AARs are more frequent (~ 40 days/year, Fig. 2B) in the Northern Hemisphere than in the Southern Hemisphere owing to the emissions of SO₂ from biogenic and anthropogenic activities over China, Europe, and the eastern US (Chakraborty et al., 2022). In the Southern Hemisphere, major transport pathways of SU AARs include regions from the southern edges of the global rainforests to the South Indian, South Atlantic, and Southern Oceans. Global rainforests and boreal forests form many BC and OC rivers due to biomass burning (Figs. 2C and 2D). Other regions of high AAR activities are noted over the

industrialized areas over eastern China, north India, Europe, eastern US where 20-40 BC or OC AAR days are observed annually.

To illustrate the overall impacts of AARs on the $PM_{2.5}$ levels over the US, we use the $PM_{2.5}$ measurements of the IMPROVE network between 1997-2020. Figure 3A-3D show the fraction of the time when AARs are associated with extreme $PM_{2.5}$ over various stations in the US. Here, extremes are defined as $PM_{2.5}$ concentration over a station greater than $15\mu g m^{-3}$. Figure 3A shows that the DU AARs are associated ~20% of the extreme $PM_{2.5}$ values over most of the US, except in the southwest US over Arizona, New Mexico, Colorado, and Utah where the association can be as high as 50% – presumably because of the DU AARs are at least in part generated from the desert and drylands in these regions. Over the stations located west of the Rocky Mountains, SU AARs are associated 20-50% of the extreme $PM_{2.5}$ values. However, the association increases to 30-70% over the stations east of the Rocky Mountain because many of the SU AARs are generated over the eastern US (Fig. 2B). OC and BC AARs are also responsible for poor air quality events, up to 70% of the extreme $PM_{2.5}$ values exhibited by the stations in the Midwest US. Apart from those generated over the US due to wildfire as shown in Figure 1, many OC and BC AARs travel from Asia (Fig. 2C and 2D) and can degrade US air quality. OC and BC AARs are strongly (up to 70%) associated with poor air quality events over stations located in the Midwest US region, where the anthropogenic and industrial emission is less. On the other hand, stations located over the west coast show a lower association (~10-20%, except ~50% in Los Angeles) between extreme $PM_{2.5}$ values and OC and BC AARs. This indicates that the high $PM_{2.5}$ levels over there are due to local emissions from industrial activities and anthropogenic emissions from the major cities located in the west coast region rather than long-range transport.

In order to explore the relationship between AARs and PM_{2.5} levels, we evaluate the ranking of the extreme PM_{2.5} levels (shading) and associated PM_{2.5} values (bubble size) over these stations. Figure 3E shows that few stations over the Southwest US, where the association between DU AARs and PM_{2.5} level was observed to be higher, are identified with red bubbles - denoting that AARs are associated with the strongest (rank 1) or the second strongest (rank 2) PM_{2.5} values recorded during the analysis period over those stations (Note that the daily PM_{2.5} records consist of 104 values or more). Stations with orange (green) colored bubble indicates the AARs were associated with the third strongest to the fifth strongest or rank 3-5 (sixth highest to ninth highest or rank 6-9) PM_{2.5} values recorded by those stations. Most of the stations in the US show that the DU AARs are associated with ranks weaker than 9 - similar to the weaker association between DU AARs and the PM_{2.5} levels.

Our results show that the ranking of SU, OC, and BC AARs with the elevated PM_{2.5} levels is stronger than that of DU AARs (Figs. 3F-3H). Although the overall association between SU AARs and high PM_{2.5} levels is weak over the regions west of the Rocky Mountains (Fig. 3B), the association tends to produce the top-ranked PM_{2.5} levels there (red bubbles, Fig. 3F). The SU AAR-associated PM_{2.5} levels are also top-ranked over the states over the eastern US, where the overall association between SU AARs and PM_{2.5} levels is strong. The size of the bubbles denotes the corresponding extreme PM_{2.5} values at that rank. For example, the bubble size over the Kalmiopsis station in Oregon shows the highest ever recorded PM_{2.5} value (186 μgm^{-3} , rank =1) over the US as shown in the case study (Fig. 1C). OC and BC AARs are often associated with the strongest or the second strongest PM_{2.5} values over most of the stations located on the west coast, Midwest, southwest, and east coast of the US (Fig. 3G and 3H).

AARs and the elevated AOD levels over the globe

In order to get a global picture of the relationships between AARs and poor air quality events, we analyze the association of the extremely high ($\text{AOD} > 98^{\text{th}}$ percentile between 1997-2020) fine (Fig. 4) and coarse (Fig. S4) mode (O'Neill et al., 2003) AOD values observed over various AERONET stations, since the availability of PM_{2.5} measurements over the globe is scarce. See Figure S3 for the 98th percentile limits of fine and coarse mode AOD values between 1997-2020. Stations with at least 10 years of level 2 data between 1997-2020 have been included in the analysis. The association of DU AARs with extreme fine-mode AOD values is relatively weak (~20%) over most of the stations except the Sahel and the Caribbean regions, where the association can reach up to 80%. In addition, the association is very high (~80%) over the Sahel and the Caribbean regions, Europe, and east Asia when we consider extreme coarse-mode AOD values (Fig. S4A). On the other hand, SU AARs are often associated (40-80%) with high fine-mode AOD values over many regions of the world, such as the eastern US, Europe, and east Asia (Fig. 4B). For extreme fine-mode AOD values, OC and BC aerosols have the highest association over various regions of the globe (Figs. 4C-4D). Such regions include the western US, east coast of the US, Amazonia, the south African region as well as Madagascar, the Ascension Island (because of the AARs generated from the Congo rainforest; Figs. 2C and 2D) in the tropical Atlantic Ocean, and east Asia. On the contrary, the association of SU, OC, and BC AARs with high coarse-mode AOD values is weaker (Figs. S4B-S4D). The size of the bubbles represents the average number of AARs observed per year between 1997-2020 over the stations shown in Figure 2.

Although DU AARs are not frequently associated with extreme fine-mode AOD values, the DU AAR-associated fine-mode AOD values attain the top ranks (rank 1 or 2) over many regions of the world including the eastern US, western Europe, Sahel region, south African countries,

and Japan (Fig. 4E). For coarse-mode AOD, the ranks are stronger over almost entire European continent, the middle-east region, east Asia, Indian subcontinent, and the Caribbean region (Fig. S5A). The red bubbles in Figures 4B-4D show that SU, OC, and BC AARs occupy the strongest ranks over almost all the stations in the world.

We also compare the association of AARs and extreme AOD values from AERONET stations (bubbles), MERRA-2 (Fig. S6), and the Moderate Resolution Imaging Spectroradiometer or MODIS satellite (Fig. S7). Figure S7 shows a reasonable agreement between the association of AARs with high AERONET AOD (AOD_A , coarse mode for DU AARs and fine mode for others), high MODIS AOD (AOD_{MO}), and MERRA-2 AOD (AOD_{ME} , Fig. S6) over the AERONET stations and their surrounding regions. AOD_{ME} (Fig. S6) appears to be lower than AOD_{MO} (Fig. S7). Figure S8 shows associated biases, root mean squared errors (RMSE), Pearson's correlation coefficient, associated significant level (p values) between AOD_A (X-axis) and AOD_{MO} as well as AOD_{ME} (Y-axis) over the AERONET stations. AOD_{ME} and AOD_A have a higher correlation than that between AOD_{MO} and AOD_A for all the species of aerosols. However, AOD_{ME} shows higher biases for all the species. RMSE values are also higher for the AOD_{ME} for DU and OC AARs.

Socio-economic impacts

The objective of this study is to show the connection between the AAR's impacts by estimating the association and intensity (in terms of ranks) with the $PM_{2.5}$ levels, which is directly related to respiratory health, in the US. We also extend the study on a global perspective by using a proxy of aerosols - AOD measured over various in-situ AERONET stations. Our findings show the impact of AARs on the poor $PM_{2.5}$ and AOD levels over the United States and the globe, respectively. AARs significantly elevate the $PM_{2.5}$ levels over various locations in the

US and are associated with $PM_{2.5}$ values above the WHO daily limit (up to 70-80% of the time). AARs are associated with extremely high AOD levels over various locations around the globe. Such association can be as high as 80% of the time. Not only that, the top-ranked (rank 1-2) $PM_{2.5}$ and AOD levels for the whole records (1997-2020) are often associated with long-range transport by AARs. Over the US, the association and the rank of the AARs with the extreme $PM_{2.5}$ and AOD levels are in tandem with each other. For example, SU AARs have an overall stronger (weaker) association with the $PM_{2.5}$ (Fig. 3B) and AOD (Fig. 4B) levels over the eastern (western) US, but they produced the top-ranked events (rank 1-2) over both regions (Figs. 3F and 4F).

Such a strong association between AARs and extreme $PM_{2.5}$ /AOD occurrences and ranks found in our study show only 30-40 AAR days each year can have significant impacts on the air quality and visibility – factors that cause millions of deaths each year. Such poor air quality events due to long-range aerosol transport, often unnoticed to the people in the receptor region, can have severe impacts on the medical industries by causing them billions of dollars. For example, the 2019-2020 wildfire season in Australia caused smoke-related $PM_{2.5}$ induced health costs of AU\$1.95 billion. The real-time aerosol product using the nature run of the GOES FP system that provides analysis and forecast products can be used to detect the real-time AAR events. Thus, poor air quality warnings can be issued in real-time for AAR related elevated $PM_{2.5}$ events and precautionary measures can be used to prevent lung disease and deaths.

The interactions between the long-range aerosol transport and poor air quality events have been investigated before. However, to our knowledge, no other study shows the unique assessment and insight provided in this study on the association and the rank of the poor air quality events with long-range aerosol transports, especially using long-term datasets (i.e. 1997-

2020). The insights are extremely important since this study investigates the impacts coming from extreme aerosol transport events, or AARs that have a very high aerosol content compared to other transport events (Chakraborty et al., 2022) . The concept might also be useful and shows promises to further study the extreme air quality events associated with AARs. Future studies based on the database created for AARs (Chakraborty et al., 2021)

(<https://doi.org/10.25346/S6/CXO9PD>) can include the real-time air quality impacts due to AARs, investigating the health impacts and death related during such events, the role of local environmental factors on poor quality events and long-range transport as well local emissions, and the assessing the monetary impacts to the medical industries including the hospitals and the insurance companies. It is important to know that despite SU AARs also travel from the East Asian region like OC and BC AARs, they do not have a higher association with the $PM_{2.5}$ levels over the Midwest region like OC and BC AARs have. SU AARs have a higher association over the stations east of the Rocky Mountains – located relatively closer to the source region compared to those SU AARs travelling from East Asia to the Midwest region. Studies involving chemical analysis and aging are needed in the future to understand the reason behind that.

Methods

A widely used AR detecting algorithm has been modified to detect narrow and elongated regions of high IAT values associated with AARs. The AAR detection algorithm is applied to IAT from the MERRA-2 reanalysis (Buchard et al., 2017; Global Modeling and Assimilation Office, 2015b, 2015a; Randles et al., 2017). For $PM_{2.5}$ measurements from the IMPROVE network and cloud-screened version 2 AOD values from AERONET stations, we choose stations with at least 10 years of data between 1997-2020 since the AAR database ranges between 1997-2020. Both the datasets are well validated and have previously been used for scientific studies

(Aldabash et al., 2020; Balarabe et al., 2015; Eck et al., 2005; Gueymard & Yang, 2020; Hwang & Hopke, 2007; Qiao et al., 2021; Sorek-Hamer et al., 2013). We first extract the dates when $PM_{2.5}$ and AOD values are higher than the WHO daily limit and above the 98th percentiles of the AOD values between 1997-2020, respectively. Then we compute how many of those days AARs have been observed over the stations and compute the fractional association (η_{AAR}) as:

$$\eta_{AAR} = \eta_{AARdays}(PM_{2.5} > 15) / \eta_{days}(PM_{2.5} > 15)$$

The rank of the association is calculated by finding the position of the maximum $PM_{2.5}$ or AOD values during AAR days relative to the $PM_{2.5}$ or AOD values during all the data records. We have calculated a similar association between MODIS and MERRA-2 AOD at every grid point. We have used daily level 3 gridded MOD08 and version 2 (MODIS Science Team, 2014) of the MERRA-2 aerosol reanalysis (Gelaro et al., 2017) dataset for the AOD information. For details of the datasets used in this study, please see Table S1 in the supplementary section.

Acknowledgement

This work was supported by the National Aeronautics and Space Administration. The contribution of S.C. and D.W. was carried out on behalf of the Jet Propulsion Laboratory, California Institute of Technology, under a contract with NASA. No new dataset has been developed in this study. Also, details about the dataset have been included in the supplementary section.

Open Research

All the data are publicly available and free to download. The links to the datasets are provided here: MODIS (<https://modis.gsfc.nasa.gov/data/dataproduct/mod08.php>); MERRA-2 (https://disc.gsfc.nasa.gov/datasets/M2I3NXGAS_5.12.4/summary); AAR data (<https://doi.org/10.25346/S6/CXO9PD>); IMPROVE network data

(<http://views.cira.colostate.edu/fed/>); AERONET data (https://aeronet.gsfc.nasa.gov/cgi-bin/webtool_aod_v3).

References:

- Aldabash, M., Bektas Balcik, F., & Glantz, P. (2020). Validation of MODIS C6.1 and MERRA-2 AOD Using AERONET Observations: A Comparative Study over Turkey. *Atmosphere*, 11(9), 905. <https://doi.org/10.3390/atmos11090905>
- Apte, J. S., Marshall, J. D., Cohen, A. J., & Brauer, M. (2015). Addressing Global Mortality from Ambient PM_{2.5}. *Environmental Science & Technology*, 49(13), 8057–8066. <https://doi.org/10.1021/acs.est.5b01236>
- Bae, C., Kim, B.-U., Kim, H. C., Yoo, C., & Kim, S. (2020). Long-Range Transport Influence on Key Chemical Components of PM_{2.5} in the Seoul Metropolitan Area, South Korea, during the Years 2012–2016. *Atmosphere*, 11(1), 48. <https://doi.org/10.3390/atmos11010048>
- Balarabe, M., Abdullah, K., & Nawawi, M. (2015). Seasonal Variations of Aerosol Optical Properties and Identification of Different Aerosol Types Based on AERONET Data over Sub-Sahara West-Africa. *Atmospheric and Climate Sciences*, 6(1), 13–28. <https://doi.org/10.4236/acs.2016.61002>
- Bell, M. L., Dominici, F., Ebisu, K., Zeger, S. L., & Samet, J. M. (2007). Spatial and Temporal Variation in PM_{2.5} Chemical Composition in the United States for Health Effects Studies. *Environmental Health Perspectives*, 115(7), 989–995. <https://doi.org/10.1289/ehp.9621>
- Buchard, V., Randles, C. A., Silva, A. M. da, Darmenov, A., Colarco, P. R., Govindaraju, R., et al. (2017). The MERRA-2 Aerosol Reanalysis, 1980 Onward. Part II: Evaluation and Case Studies. *Journal of Climate*, 30(17), 6851–6872. <https://doi.org/10.1175/JCLI-D-16-0613.1>
- Chakraborty, S., Guan, B., Waliser, D. E., da Silva, A. M., Uluatam, S., & Hess, P. (2021). Extending the Atmospheric River Concept to Aerosols: Climate and Air Quality Impacts. *Geophysical Research Letters*, 48(9), e2020GL091827. <https://doi.org/10.1029/2020GL091827>
- Chakraborty, S., Guan, B., Waliser, D. E., & da Silva, A. M. (2022). Aerosol atmospheric rivers: climatology, event characteristics, and detection algorithm sensitivities. *Atmospheric Chemistry and Physics*, 22(12), 8175–8195. <https://doi.org/10.5194/acp-22-8175-2022>
- Chen, T.-F., Chang, K.-H., & Tsai, C.-Y. (2014). Modeling direct and indirect effect of long range transport on atmospheric PM_{2.5} levels. *Atmospheric Environment*, 89, 1–9. <https://doi.org/10.1016/j.atmosenv.2014.01.065>
- Clappier, A., Pisoni, E., & Thunis, P. (2015). A new approach to design source–receptor relationships for air quality modelling. *Environmental Modelling & Software*, 74, 66–74. <https://doi.org/10.1016/j.envsoft.2015.09.007>
- Eck, T. F., Holben, B. N., Dubovik, O., Smirnov, A., Goloub, P., Chen, H. B., et al. (2005). Columnar aerosol optical properties at AERONET sites in central eastern Asia and

- aerosol transport to the tropical mid-Pacific. *Journal of Geophysical Research: Atmospheres*, 110(D6). <https://doi.org/10.1029/2004JD005274>
- Gelaro, R., McCarty, W., Suárez, M. J., Todling, R., Molod, A., Takacs, L., et al. (2017). The Modern-Era Retrospective Analysis for Research and Applications, Version 2 (MERRA-2). *Journal of Climate*, 30(14), 5419–5454. <https://doi.org/10.1175/JCLI-D-16-0758.1>
- Global Modeling and Assimilation Office, G. (2015a). GES DISC Dataset: MERRA-2 tavg1_2d_aer_Nx: 2d,1-Hourly,Time-averaged,Single-Level,Assimilation,Aerosol Diagnostics V5.12.4 (M2T1NXAER 5.12.4). Retrieved April 20, 2023, from https://disc.gsfc.nasa.gov/datasets/M2T1NXAER_5.12.4/summary
- Global Modeling and Assimilation Office, G. (2015b). GES DISC Dataset: MERRA-2 tavgU_2d_adg_Nx: 2d,diurnal,Time-averaged,Single-Level,Assimilation,Aerosol Diagnostics (extended) V5.12.4 (M2TUNXADG 5.12.4). Retrieved April 20, 2023, from https://disc.gsfc.nasa.gov/datasets/M2TUNXADG_5.12.4/summary
- Guan, B., & Waliser, D. E. (2015). Detection of atmospheric rivers: Evaluation and application of an algorithm for global studies. *Journal of Geophysical Research: Atmospheres*, 120(24), 12514–12535. <https://doi.org/10.1002/2015JD024257>
- Guan, B., Waliser, D. E., & Ralph, F. M. (2020). A multimodel evaluation of the water vapor budget in atmospheric rivers. *Annals of the New York Academy of Sciences*, 1472(1), 139–154. <https://doi.org/10.1111/nyas.14368>
- Gueymard, C. A., & Yang, D. (2020). Worldwide validation of CAMS and MERRA-2 reanalysis aerosol optical depth products using 15 years of AERONET observations. *Atmospheric Environment*, 225, 117216. <https://doi.org/10.1016/j.atmosenv.2019.117216>
- Guo, H., Kota, S. H., Sahu, S. K., & Zhang, H. (2019). Contributions of local and regional sources to PM_{2.5} and its health effects in north India. *Atmospheric Environment*, 214, 116867. <https://doi.org/10.1016/j.atmosenv.2019.116867>
- Han, L., Cheng, S., Zhuang, G., Ning, H., Wang, H., Wei, W., & Zhao, X. (2015). The changes and long-range transport of PM_{2.5} in Beijing in the past decade. *Atmospheric Environment*, 110, 186–195. <https://doi.org/10.1016/j.atmosenv.2015.03.013>
- Holben, B. N., Eck, T. F., Slutsker, I., Tanré, D., Buis, J. P., Setzer, A., et al. (1998). AERONET—A Federated Instrument Network and Data Archive for Aerosol Characterization. *Remote Sensing of Environment*, 66(1), 1–16. [https://doi.org/10.1016/S0034-4257\(98\)00031-5](https://doi.org/10.1016/S0034-4257(98)00031-5)
- Hwang, I., & Hopke, P. K. (2007). Estimation of source apportionment and potential source locations of PM_{2.5} at a west coastal IMPROVE site. *Atmospheric Environment*, 41(3), 506–518. <https://doi.org/10.1016/j.atmosenv.2006.08.043>
- Karaca, F., Anil, I., & Alagha, O. (2009). Long-range potential source contributions of episodic aerosol events to PM₁₀ profile of a megacity. *Atmospheric Environment*, 43(36), 5713–5722. <https://doi.org/10.1016/j.atmosenv.2009.08.005>
- Kong, S., Han, B., Bai, Z., Chen, L., Shi, J., & Xu, Z. (2010). Receptor modeling of PM_{2.5}, PM₁₀ and TSP in different seasons and long-range transport analysis at a coastal site of Tianjin, China. *The Science of the Total Environment*, 408(20), 4681–4694. <https://doi.org/10.1016/j.scitotenv.2010.06.005>
- Lang, J., Zhang, Y., Zhou, Y., Cheng, S., Chen, D., Guo, X., et al. (2017). Trends of PM_{2.5} and Chemical Composition in Beijing, 2000–2015. *Aerosol and Air Quality Research*, 17(2), 412–425. <https://doi.org/10.4209/aaqr.2016.07.0307>

- Li, D., Liu, J., Zhang, J., Gui, H., Du, P., Yu, T., et al. (2017). Identification of long-range transport pathways and potential sources of PM_{2.5} and PM₁₀ in Beijing from 2014 to 2015. *Journal of Environmental Sciences (China)*, 56, 214–229. <https://doi.org/10.1016/j.jes.2016.06.035>
- Li, R., Zhou, R., & Zhang, J. (2018). Function of PM_{2.5} in the pathogenesis of lung cancer and chronic airway inflammatory diseases. *Oncology Letters*, 15(5), 7506–7514. <https://doi.org/10.3892/ol.2018.8355>
- Lin, C.-Y., Liu, S. C., Chou, C. C.-K., Huang, S.-J., Liu, C.-M., Kuo, C.-H., & Young, C.-Y. (2005). Long-range transport of aerosols and their impact on the air quality of Taiwan. *Atmospheric Environment*, 39(33), 6066–6076. <https://doi.org/10.1016/j.atmosenv.2005.06.046>
- MODIS Science Team. (2014). MYD08_M3 MODIS/Aqua Aerosol Cloud Water Vapor Ozone Monthly L3 Global 1Deg CMG [Data set]. NASA Level 1 and Atmosphere Archive and Distribution System. https://doi.org/10.5067/MODIS/MYD08_M3.006
- O'Neill, N. T., Eck, T. F., Smirnov, A., Holben, B. N., & Thulasiraman, S. (2003). Spectral discrimination of coarse and fine mode optical depth. *Journal of Geophysical Research (Atmospheres)*, 108, 4559. <https://doi.org/10.1029/2002JD002975>
- Perrone, M. R., Becagli, S., Garcia Orza, J. A., Vecchi, R., Dinoi, A., Udusti, R., & Cabello, M. (2013). The impact of long-range-transport on PM₁ and PM_{2.5} at a Central Mediterranean site. *Atmospheric Environment*, 71, 176–186. <https://doi.org/10.1016/j.atmosenv.2013.02.006>
- Prospero, J. M. (1999). Long-term measurements of the transport of African mineral dust to the southeastern United States: Implications for regional air quality. *Journal of Geophysical Research: Atmospheres*, 104(D13), 15917–15927. <https://doi.org/10.1029/1999JD900072>
- Qiao, X., Zhang, Q., Wang, D., Hao, J., & Jiang, J. (2021). Improving data reliability: A quality control practice for low-cost PM_{2.5} sensor network. *Science of The Total Environment*, 779, 146381. <https://doi.org/10.1016/j.scitotenv.2021.146381>
- Randles, C. A., Silva, A. M. da, Buchard, V., Colarco, P. R., Darmenov, A., Govindaraju, R., et al. (2017). The MERRA-2 Aerosol Reanalysis, 1980 Onward. Part I: System Description and Data Assimilation Evaluation. *Journal of Climate*, 30(17), 6823–6850. <https://doi.org/10.1175/JCLI-D-16-0609.1>
- Saliba, N. A., Kouyoumdjian, H., & Roumié, M. (2007). Effect of local and long-range transport emissions on the elemental composition of PM_{10-2.5} and PM_{2.5} in Beirut. *Atmospheric Environment*, 41(31), 6497–6509. <https://doi.org/10.1016/j.atmosenv.2007.04.032>
- Shimadera, H., Kojima, T., & Kondo, A. (2016). Evaluation of Air Quality Model Performance for Simulating Long-Range Transport and Local Pollution of PM_{2.5} in Japan. *Advances in Meteorology*, 2016, e5694251. <https://doi.org/10.1155/2016/5694251>
- Sitnov, S. A., Mokhov, I. I., & Likhoshesterova, A. A. (2020). Exploring large-scale black-carbon air pollution over Northern Eurasia in summer 2016 using MERRA-2 reanalysis data. *Atmospheric Research*, 235, 104763. <https://doi.org/10.1016/j.atmosres.2019.104763>
- Solomon, P. A., Crumpler, D., Flanagan, J. B., Jayanty, R. K. M., Rickman, E. E., & McDade, C. E. (2014). U.S. national PM_{2.5} Chemical Speciation Monitoring Networks-CSN and IMPROVE: description of networks. *Journal of the Air & Waste Management Association (1995)*, 64(12), 1410–1438. <https://doi.org/10.1080/10962247.2014.956904>
- Sorek-Hamer, M., Strawa, A. W., Chatfield, R. B., Esswein, R., Cohen, A., & Broday, D. M. (2013). Improved retrieval of PM_{2.5} from satellite data products using non-linear

- methods. *Environmental Pollution (Barking, Essex: 1987)*, 182, 417–423.
<https://doi.org/10.1016/j.envpol.2013.08.002>
- Squizzato, S., Masiol, M., Innocente, E., Pecorari, E., Rampazzo, G., & Pavoni, B. (2012). A procedure to assess local and long-range transport contributions to PM_{2.5} and secondary inorganic aerosol. *Journal of Aerosol Science*, 46, 64–76.
<https://doi.org/10.1016/j.jaerosci.2011.12.001>
- Todorović, M. N., Radenković, M. B., Onjia, A. E., & Ignjatović, L. M. (2020). Characterization of PM_{2.5} sources in a Belgrade suburban area: a multi-scale receptor-oriented approach. *Environmental Science and Pollution Research International*, 27(33), 41717–41730.
<https://doi.org/10.1007/s11356-020-10129-z>
- Uranishi, K., Ikemori, F., Shimadera, H., Kondo, A., & Sugata, S. (2019). Impact of field biomass burning on local pollution and long-range transport of PM_{2.5} in Northeast Asia. *Environmental Pollution*, 244, 414–422. <https://doi.org/10.1016/j.envpol.2018.09.061>
- Wang, L., Liu, Z., Sun, Y., Ji, D., & Wang, Y. (2015). Long-range transport and regional sources of PM_{2.5} in Beijing based on long-term observations from 2005 to 2010. *Atmospheric Research*, 157, 37–48. <https://doi.org/10.1016/j.atmosres.2014.12.003>
- Xing, Y.-F., Xu, Y.-H., Shi, M.-H., & Lian, Y.-X. (2016). The impact of PM_{2.5} on the human respiratory system. *Journal of Thoracic Disease*, 8(1), E69–E74.
<https://doi.org/10.3978/j.issn.2072-1439.2016.01.19>
- Xu, X., Wu, H., Yang, X., & Xie, L. (2020). Distribution and transport characteristics of dust aerosol over Tibetan Plateau and Taklimakan Desert in China using MERRA-2 and CALIPSO data. *Atmospheric Environment*, 237, 117670.
<https://doi.org/10.1016/j.atmosenv.2020.117670>
- Ye, B., Ji, X., Yang, H., Yao, X., Chan, C. K., Cadle, S. H., et al. (2003). Concentration and chemical composition of PM_{2.5} in Shanghai for a 1-year period. *Atmospheric Environment*, 37(4), 499–510. [https://doi.org/10.1016/S1352-2310\(02\)00918-4](https://doi.org/10.1016/S1352-2310(02)00918-4)
- Zíková, N., Wang, Y., Yang, F., Li, X., Tian, M., & Hopke, P. K. (2016). On the source contribution to Beijing PM_{2.5} concentrations. *Atmospheric Environment*, 134, 84–95.
<https://doi.org/10.1016/j.atmosenv.2016.03.047>

Figures

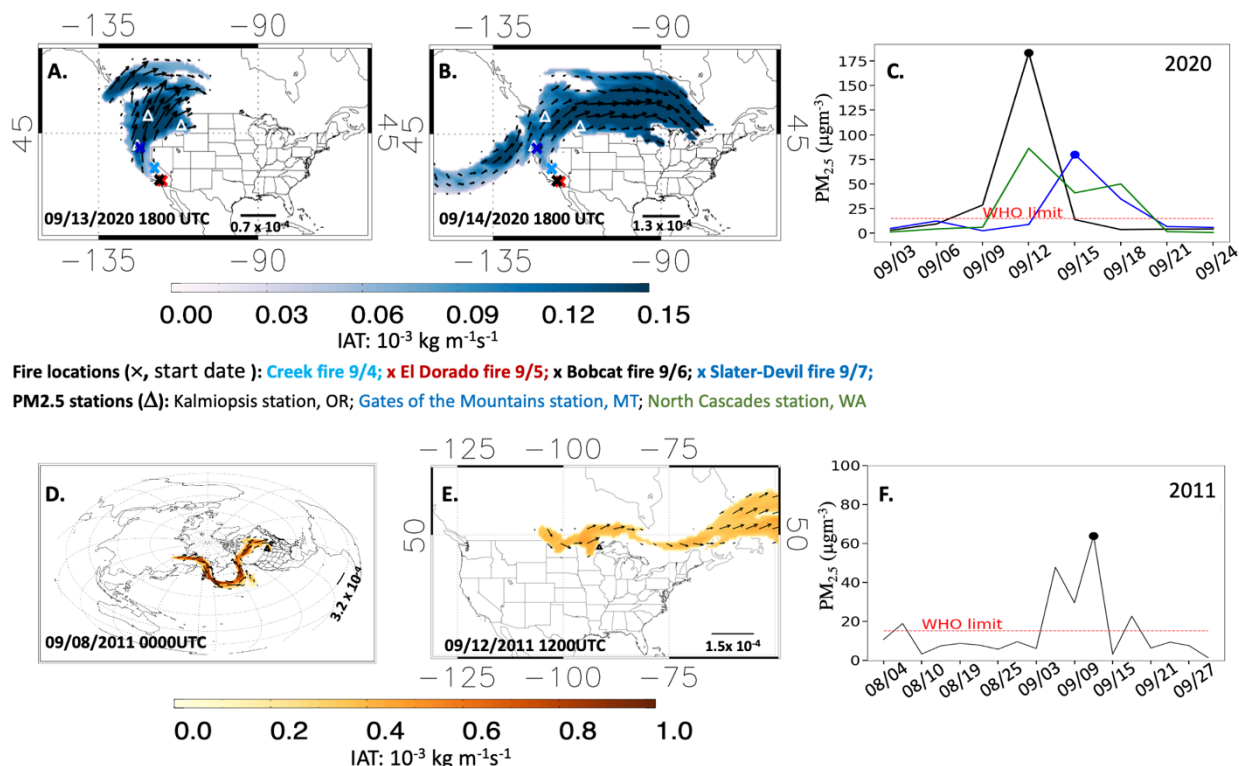


Figure1. Case studies of the impacts of AARs on PM_{2.5} levels. Figure 1 shows a Sulfate AAR generated from wild fire events in California. (A) The location of four large wildfire events with total burned area greater than 15000 acres and lasting for more than two months (marked in the map as x) on 09/13/2020 1800 UTC. The PM_{2.5} monitoring stations are marked as triangles. (B) The same river on 09/14/2020 at 1800 UTC. (C) PM_{2.5} levels monitored over the stations shown in the maps as triangles. (D) one dust AAR on 09/08/2011 at 00UTC. (E) The same river on 09/12/2011. (F) PM_{2.5} level monitored over the Boundary Water Canoe Area in MN (marked as triangle in the map) during the AAR event. Shading shows the IAT values and the arrows represent the vectors.

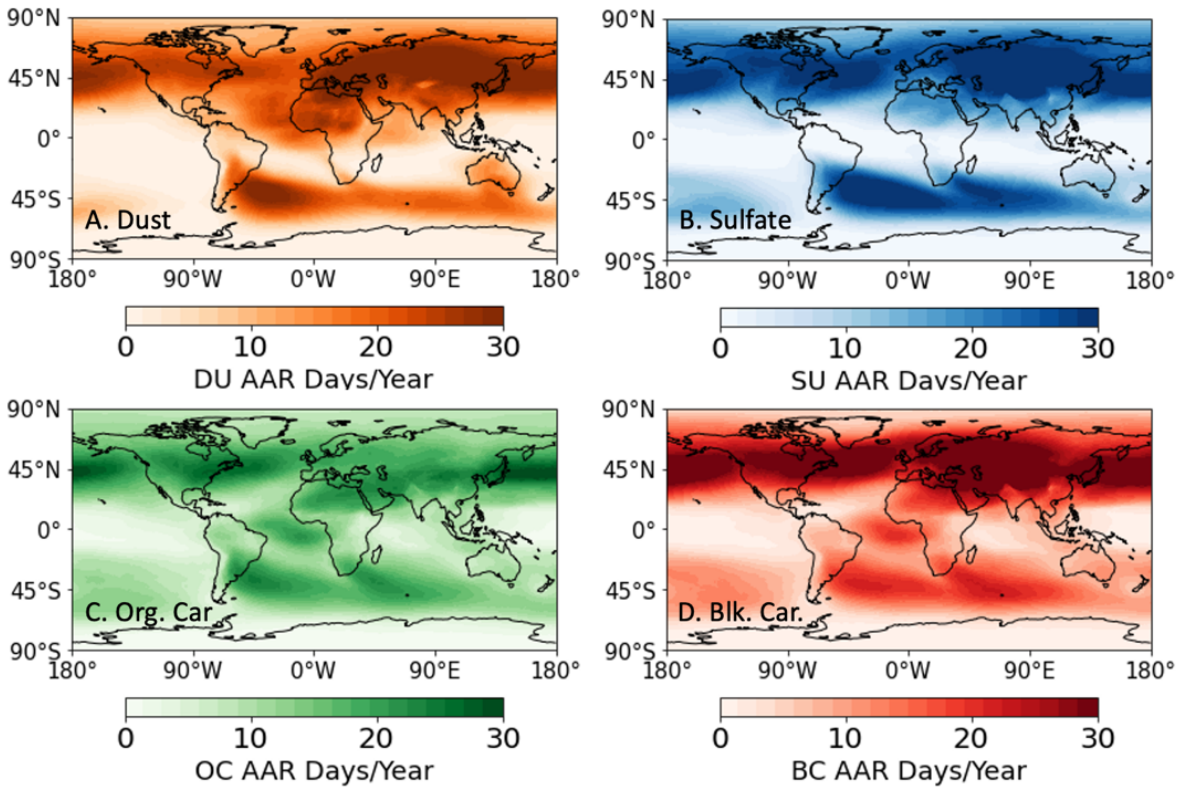


Figure 2. Maps of AAR days/year for four different species (A) dust, (B) sulfate, (C) organic carbon, and (D) black carbon between 1997-2020.

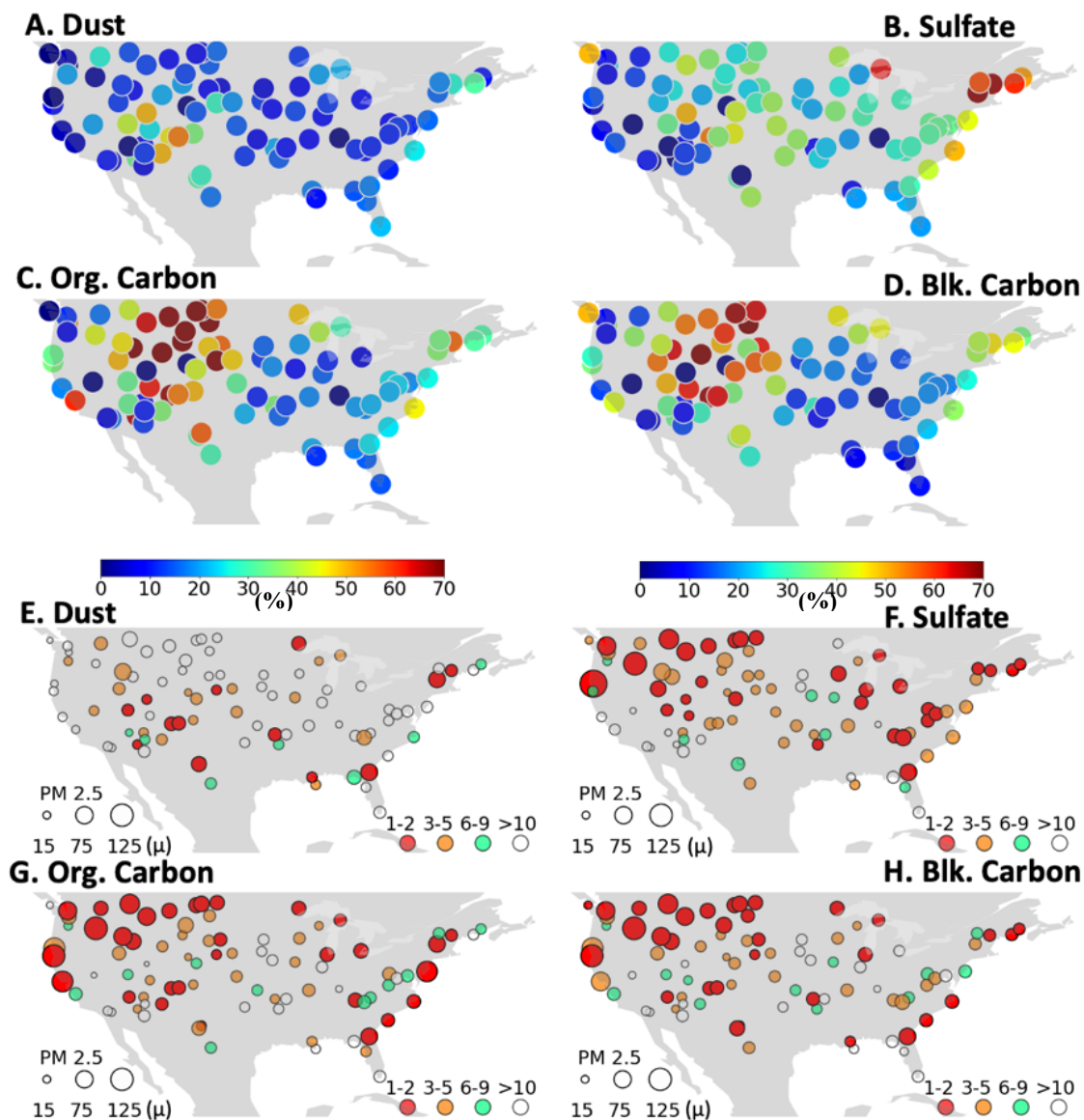


Figure 3. Fraction of extreme PM_{2.5} levels (PM_{2.5} > 15μ or WHO daily limit) associated with AAR events (shading, %) between 1997-2020 for (A) Dust, (B) Sulfate, (C) Organic Carbon, and (D) Black Carbon AARs. The highest rank (shading) of AAR related extremes associated with extreme PM_{2.5} levels for (E) Dust, (F) Sulfate, (G) Organic Carbon, and (H) Black Carbon AARs. The size of the circles shows the corresponding PM_{2.5} values at that rank.

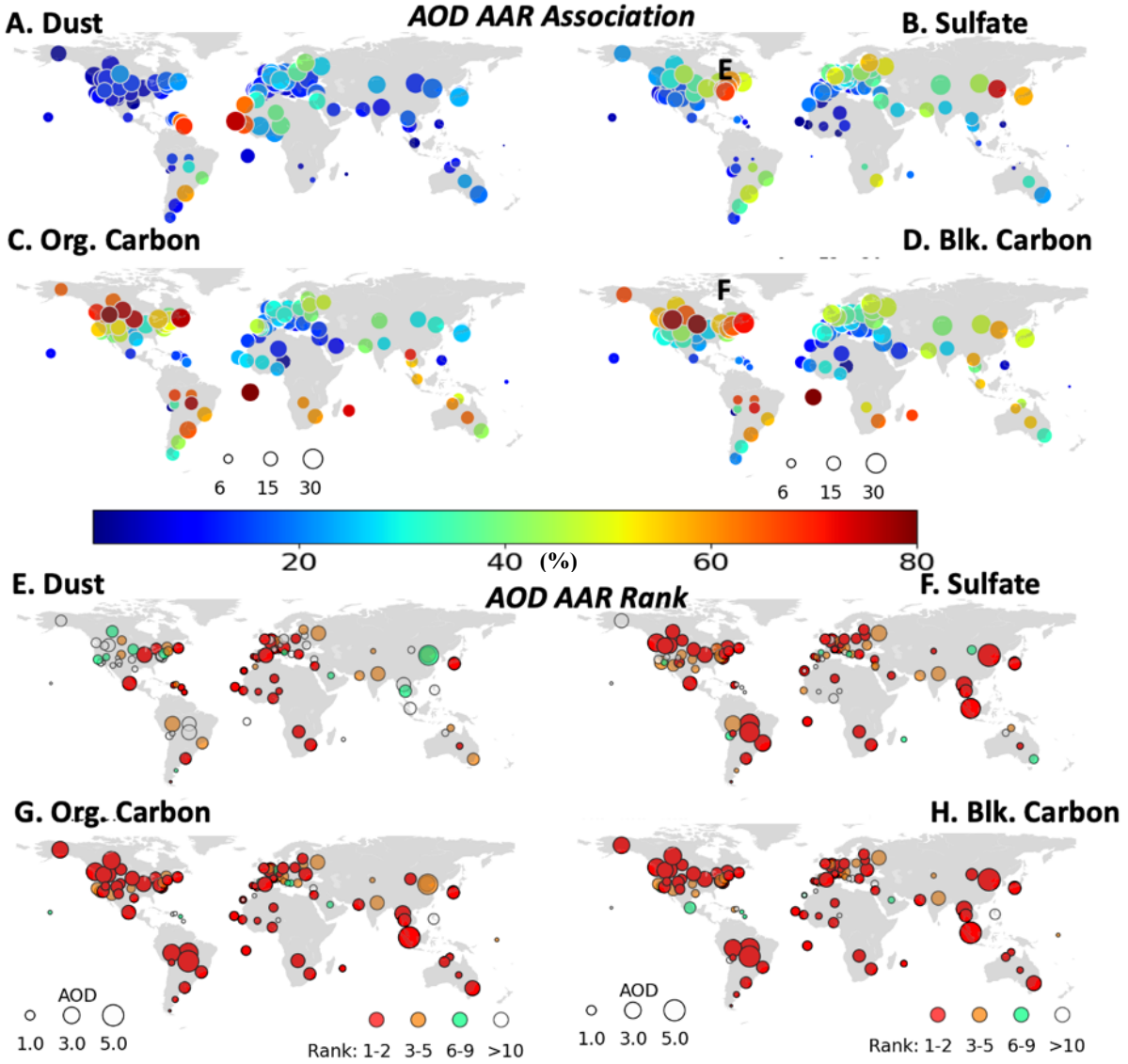


Figure 4. Fraction of extreme fine-mode AOD values ($\text{AOD} > 98^{\text{th}}$ percentile between 1997-2020) associated with AAR events (shading, %) and the AAR days/year (size of the bubbles) between 1997-2020 for (A) Dust, (B) Sulfate, (C) Organic Carbon, and (D) Black Carbon AARs. The size of the bubbles show the number of AARs observed each year over that station from Figure 2. The highest rank (shading) of AAR related extremes associated with extreme AOD values for (E) Dust, (F) Sulfate, (G) Organic Carbon, and (H) Black Carbon AARs. The size of the bubbles shows the corresponding AOD values at that rank.

Supplementary material

Aerosol Atmospheric Rivers as Drivers of Extreme Poor Air Quality Events and Record

PM_{2.5} Levels

Sudip Chakraborty^{1*}, Bin Guan^{1,2}, Duane E. Waliser¹, Arlindo M. da Silva³, Jonathan H Jiang¹

¹Jet Propulsion Laboratory, California Institute of Technology, Pasadena, CA, USA

²Joint Institute for Regional Earth System Science and Engineering, University of California, Los Angeles, CA, USA

³ Global Modeling and Assimilation Office, NASA/Goddard Space Flight Center, Greenbelt, MD, USA

*Corresponding Author email: sudip.chakraborty@jpl.nasa.gov

Supplementary Figures and Table:

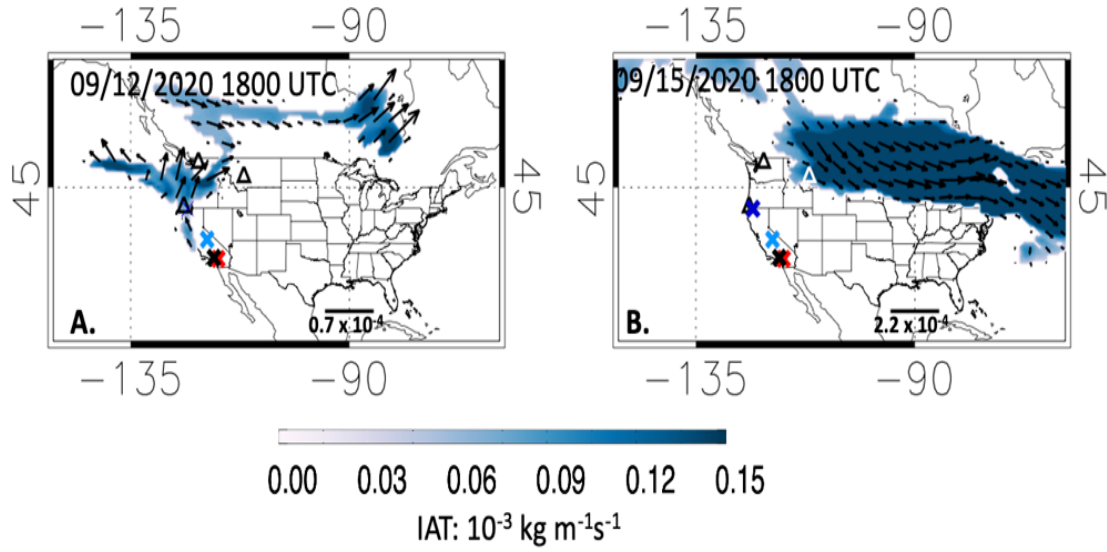


Figure S1. Same sulfate river as in Figure 1 on 09/12/2020 at 1800 UTC and (B) 09/15/2020 at 1800 UTC. Shading shows the IAT values and the arrows represent the vectors.

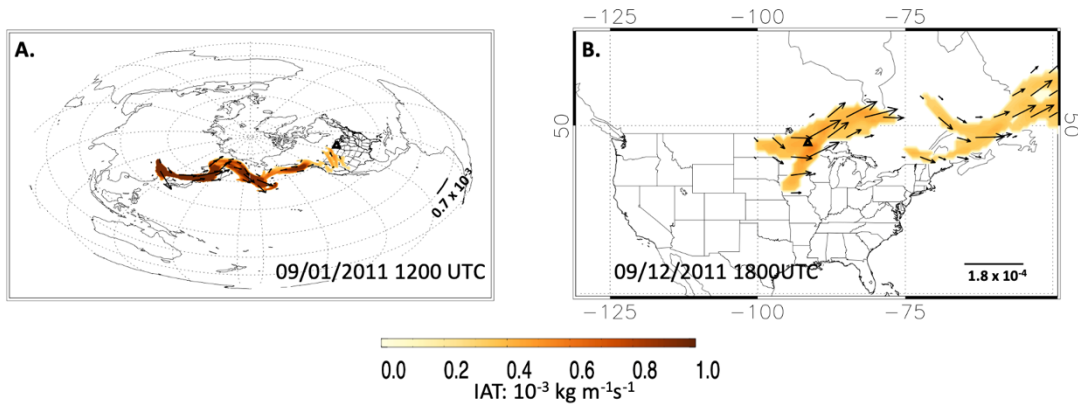


Figure S2. Same dust river as in Figure 1 on 09/01/2011 at 1200 UTC and (B) 09/12/2011 at 1800 UTC. Shading shows the IAT values and the arrows represent the vectors.

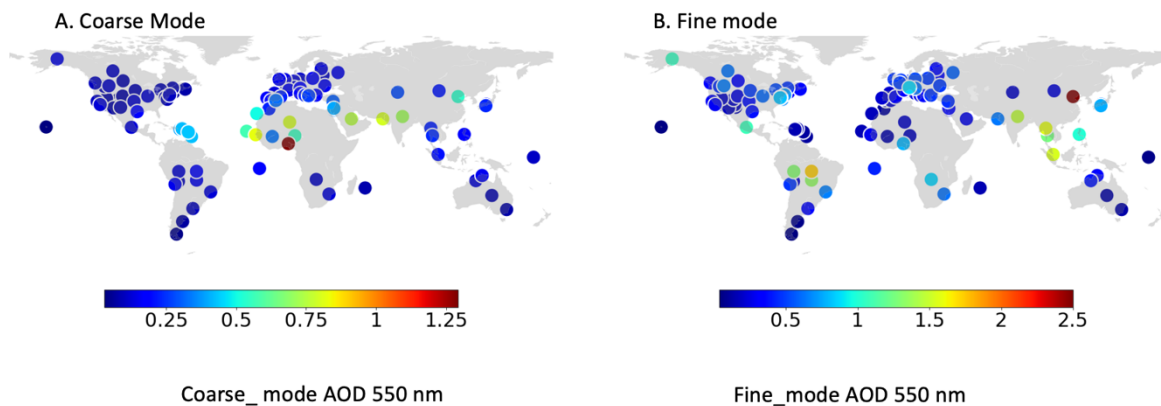


Figure S3. 98th percentile thresholds of (A) coarse mode and (B) fine mode AOD at 550 nm from AERONET stations. Each station has a minimum of 10 years of data.

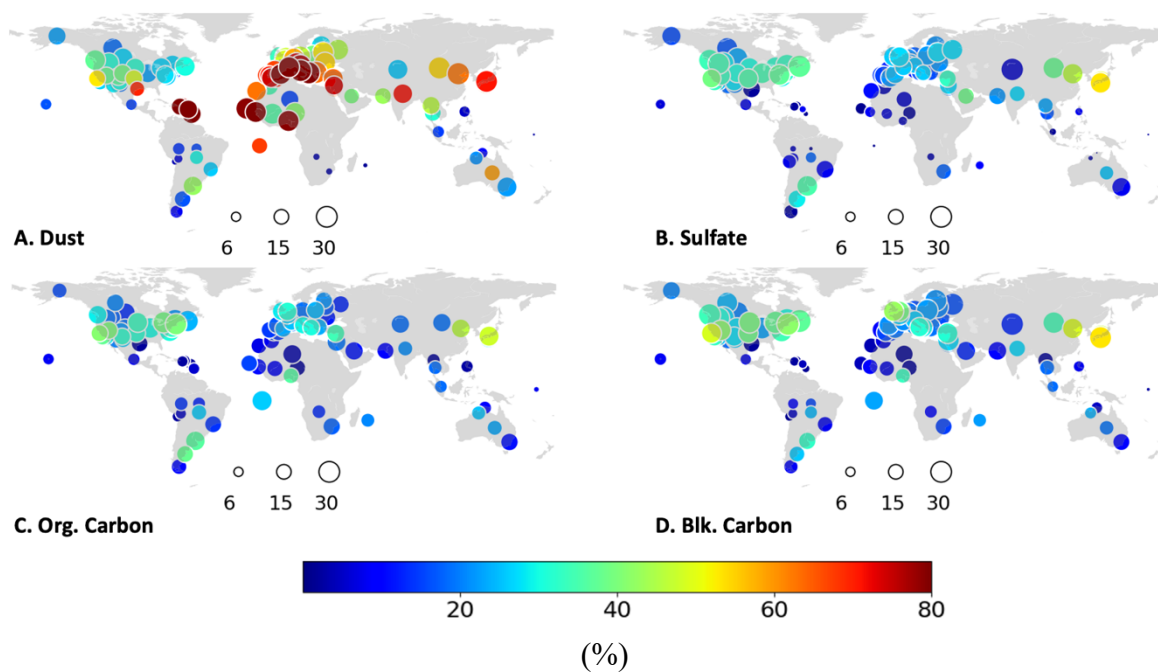


Figure S4. Same as in Figure 4 for AAR-AOD association, but for the coarse mode.

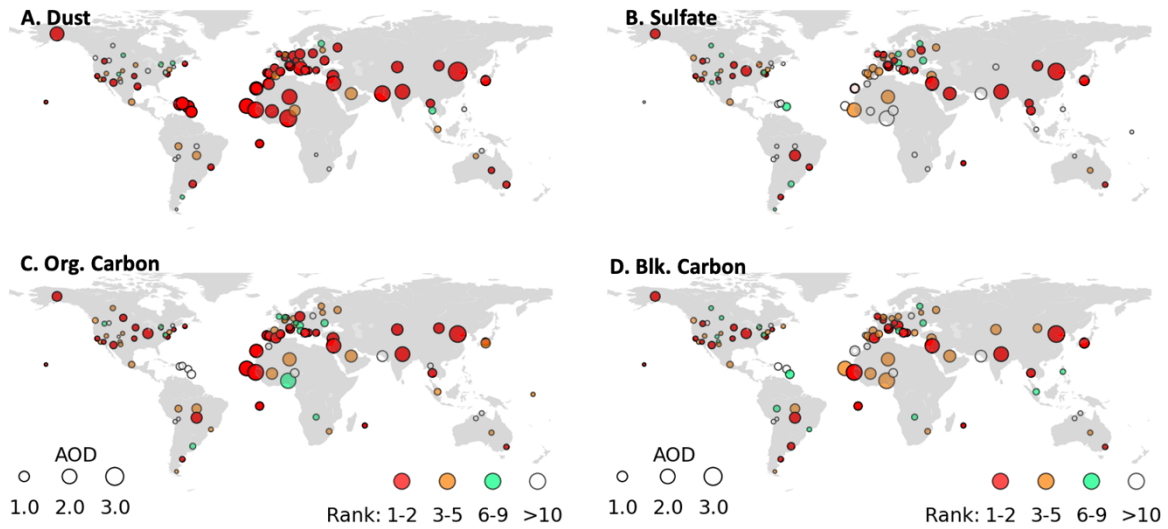


Figure S5. Same as in Figure 4 for AAR-AOD rank, but for the coarse mode.

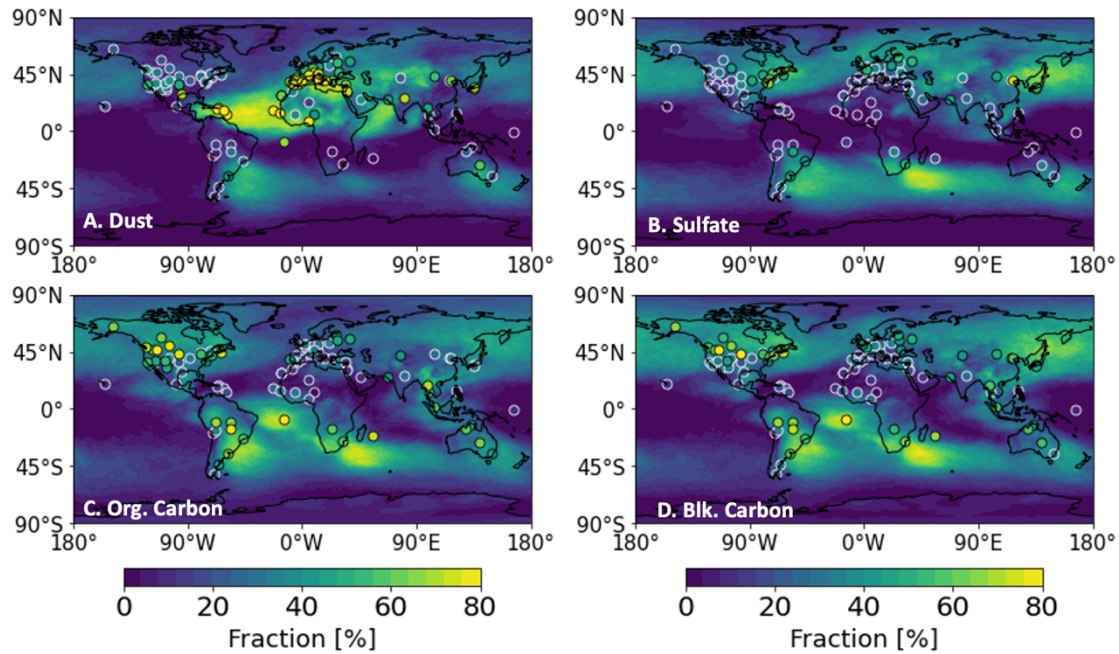


Figure S6. Fraction of extreme AOD values (AOD > 98th percentile between 1997-2020) associated with AAR events (shading, %) from MEERA-2 data between 1997-2020 for (A) Dust, (B) Sulfate, (C) Organic Carbon, and (D) Black Carbon AARs. The bubbles show the association between AARs and extreme AOD values from the AERONET stations from

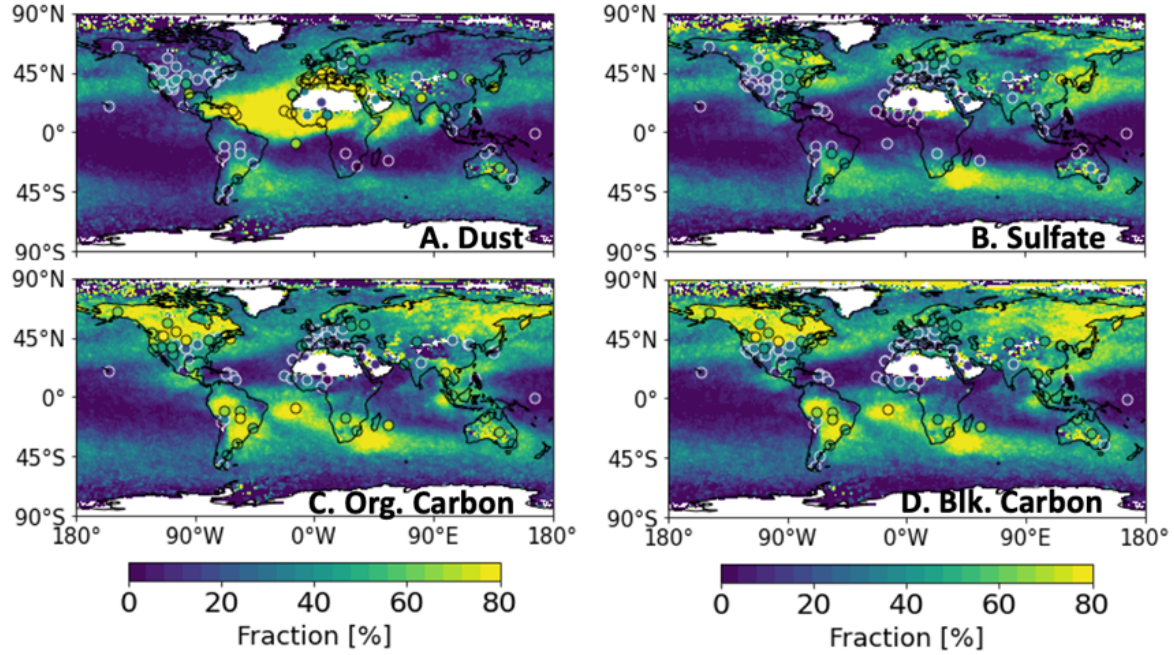


Figure S7. Same as in Figure S6 for AAR-AOD rank, but for MODIS AOD data between 2002-2020.

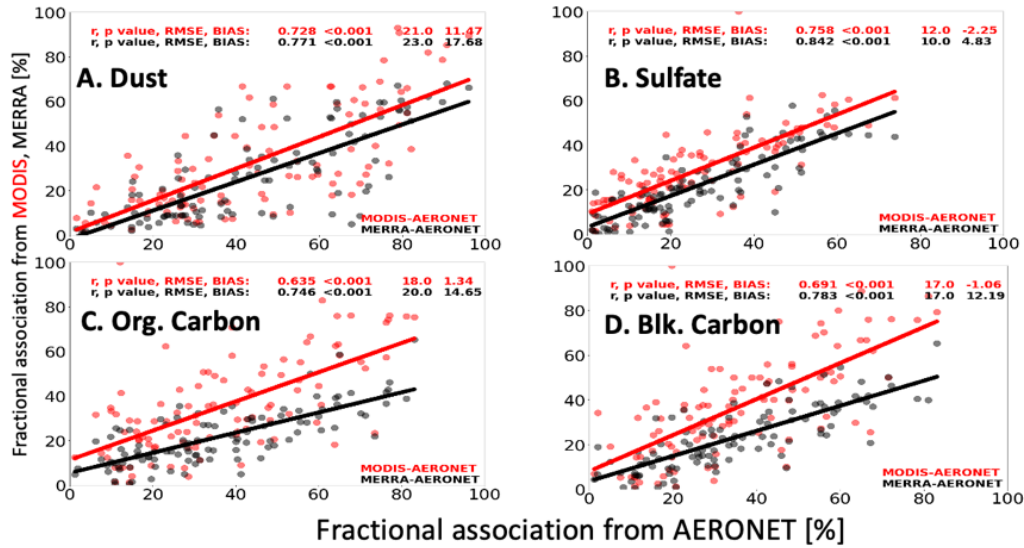


Figure S8. Scatterplots of AAR-AOD association using AERONET AOD data (X axis) and MERRA-2 / MODIS data (Y axis) over the AERONET stations. AARs association with AOD values from AERONET-MODIS (MERRA-2) are shown in red (black) color. For dust, coarse mode AOD data from AERONET stations have been used. For other species, fine mode AOD data have been used.

Supplementary Table S1: List of datasets used.

Data set	Parameter	Resolution	Version / Links to the datasets
MODIS	AOD	$1^{\circ} \times 1^{\circ}$	Daily, Level 3 MOD08 data
MERRA-2	AOD	$0.625^{\circ} \times 0.5^{\circ}$	inst3_2d_gas_Nx: 2d, 3-Hourly, Instantaneous, Single-Level, Assimilation V5.12.4 (M2I3NXGAS, https://disc.gsfc.nasa.gov/datasets/M2I3NXGAS_5.12.4/summary)
AAR data base	AAR location and shape	$0.625^{\circ} \times 0.5^{\circ}$	https://doi.org/10.25346/S6/CXO9PD
IMPROVE network	PM _{2.5}	Stations	http://views.cira.colostate.edu/fed/
AERONET data	Coarse and fine mode AOD	Stations	Version 2, https://aeronet.gsfc.nasa.gov/cgi-bin/webtool_aod_v3